Gravitational waves from Massive Primordial Black Holes as Dark Matter

based on S. Clesse & JGB, arXiv:1603.05234
S. Clesse & JGB, Phys Rev D92 (2015) 023524
JGB, Linde & Wands, Phys Rev D54 (1996) 6040

Juan García-Bellido
8th September 2016

Outline

- Discovery of 3 binary BH by aLIGO starts a new era of GW Astronomy
- Massive PBH could be the main component of Dark Matter
- Specific signatures of PBH
- Future: Testing the idea with cosmological observations
- Conclusions

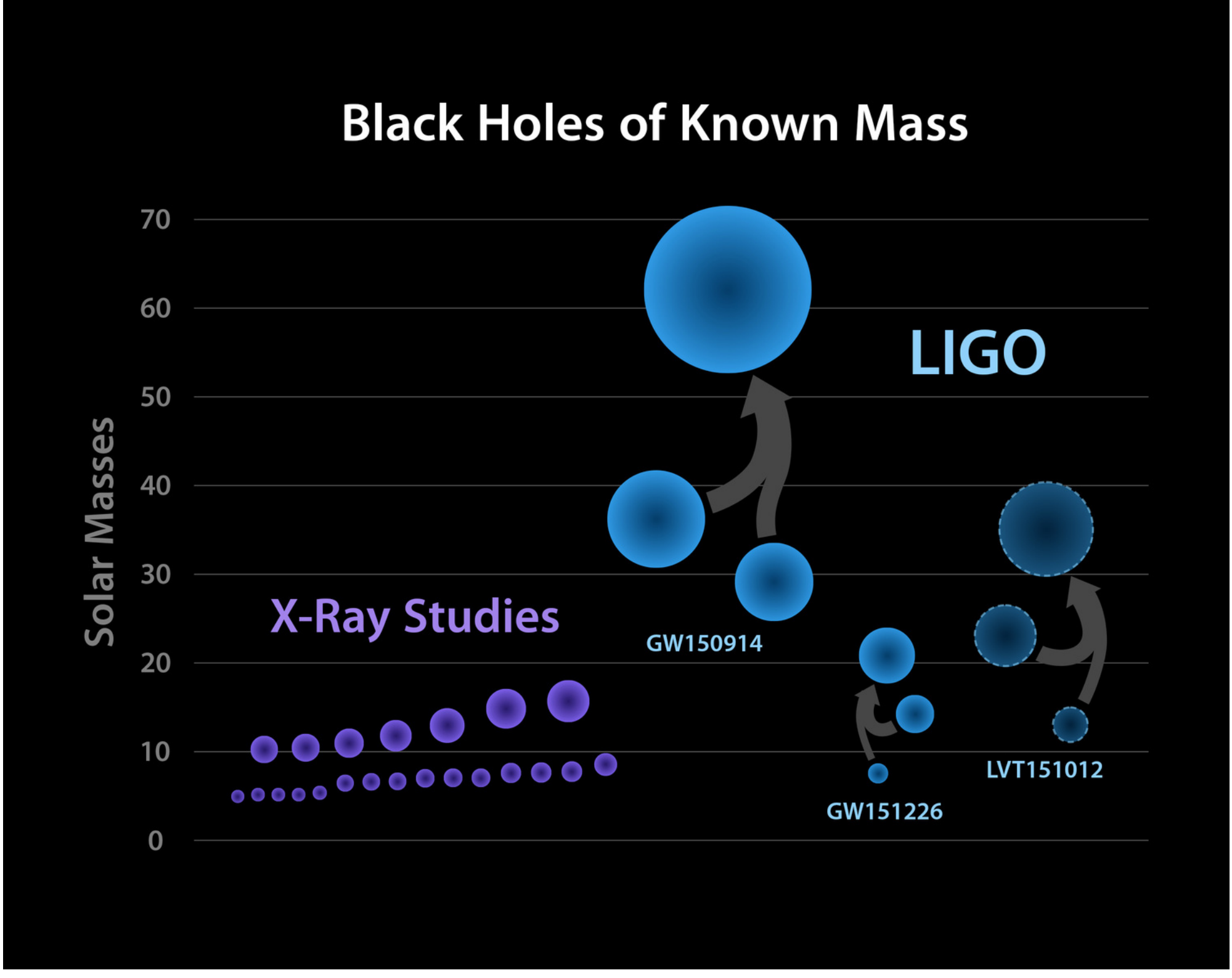
Black Holes of Known Mass
Solar Masses
70
60
50
40
30
20
10
0
X-Ray Studies
LIGO
GW150914
GW151226
LVT151012

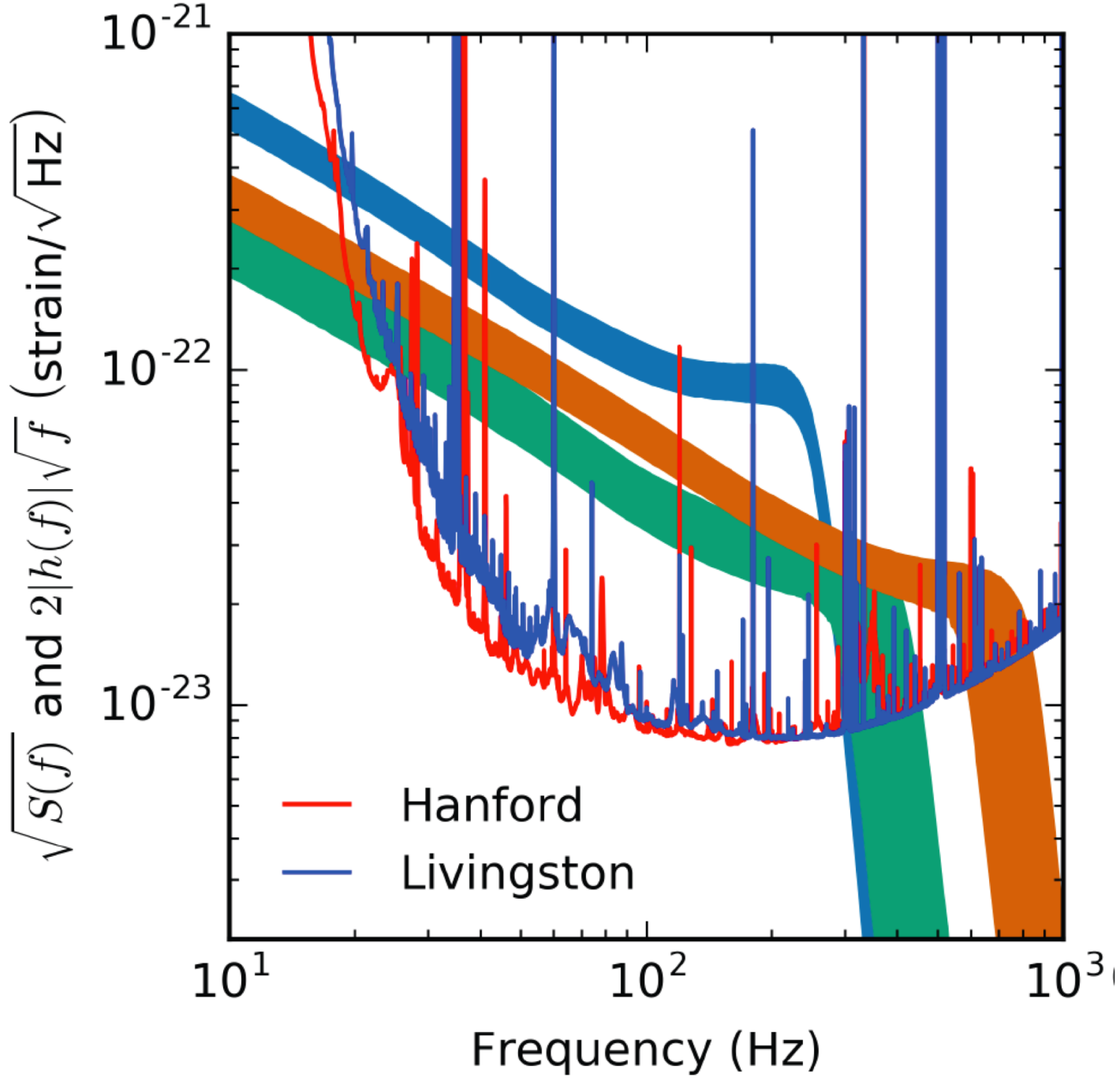
10^{-21}
10^{-22}
10^{-23}
$\sqrt{S(f)}$ and $2|h(f)|\sqrt{f}$ (strain/$\sqrt{\text{Hz}}$)
Hanford
Livingston
10^{1}
10^{2}
10^{3}
Frequency (Hz)

	GW150914			GW151226			LVT151012		
	EOBNR	IMRPhenom	Overall	EOBNR	IMRPhenom	Overall	EOBNR	IMRPhenom	Overall
Detector frame									
Total mass $M/\mathrm{M}_\odot$	$71.0^{+4.6}_{-4.0}$	$71.2^{+3.5}_{-3.2}$	$71.1^{+4.1\pm0.7}_{-3.6\pm0.8}$	$23.6^{+8.0}_{-1.3}$	$23.8^{+5.1}_{-1.5}$	$23.7^{+6.5\pm2.2}_{-1.4\pm0.1}$	45^{+17}_{-4}	44^{+12}_{-3}	$44^{+16\pm5}_{-3\pm0}$
Chirp mass $\mathscr{M}/\mathrm{M}_\odot$	$30.4^{+2.3}_{-1.6}$	$30.7^{+1.5}_{-1.5}$	$30.6^{+1.9\pm0.3}_{-1.6\pm0.4}$	$9.71^{+0.08}_{-0.07}$	$9.72^{+0.06}_{-0.06}$	$9.72^{+0.07\pm0.01}_{-0.06\pm0.01}$	$18.1^{+1.3}_{-0.9}$	$18.1^{+0.8}_{-0.8}$	$18.1^{+1.0\pm0.5}_{-0.8\pm0.1}$
Primary mass $m_1/\mathrm{M}_\odot$	$40.2^{+5.2}_{-4.8}$	$38.5^{+5.4}_{-3.3}$	$39.4^{+5.4\pm1.3}_{-4.1\pm0.2}$	$15.3^{+10.8}_{-3.8}$	$15.8^{+7.2}_{-4.0}$	$15.6^{+9.0\pm2.6}_{-4.0\pm0.2}$	29^{+23}_{-8}	27^{+19}_{-6}	$28^{+21\pm5}_{-7\pm0}$
Secondary mass $m_2/\mathrm{M}_\odot$	$30.6^{+5.1}_{-4.2}$	$32.7^{+3.1}_{-4.9}$	$31.7^{+4.0\pm0.1}_{-4.9\pm1.2}$	$8.3^{+2.5}_{-2.9}$	$8.1^{+2.5}_{-2.1}$	$8.2^{+2.6\pm0.2}_{-2.5\pm0.5}$	15^{+5}_{-6}	16^{+4}_{-6}	$16^{+5\pm0}_{-6\pm1}$
Final mass $M_\mathrm{f}/\mathrm{M}_\odot$	$67.8^{+4.0}_{-3.6}$	$67.9^{+3.2}_{-2.9}$	$67.8^{+3.7\pm0.6}_{-3.3\pm0.7}$	$22.5^{+8.2}_{-1.4}$	$22.8^{+5.3}_{-1.6}$	$22.6^{+6.7\pm2.2}_{-1.5\pm0.1}$	43^{+17}_{-4}	42^{+13}_{-2}	$42^{+16\pm5}_{-3\pm0}$
Source frame									
Total mass $M^\mathrm{source}/\mathrm{M}_\odot$	$65.5^{+4.4}_{-3.9}$	$65.1^{+3.6}_{-3.1}$	$65.3^{+4.1\pm1.0}_{-3.4\pm0.3}$	$21.6^{+7.4}_{-1.6}$	$21.9^{+4.7}_{-1.7}$	$21.8^{+5.9\pm2.0}_{-1.7\pm0.1}$	38^{+15}_{-5}	37^{+11}_{-4}	$37^{+13\pm4}_{-4\pm0}$
Chirp mass $\mathscr{M}^\mathrm{source}/\mathrm{M}_\odot$	$28.1^{+2.1}_{-1.6}$	$28.1^{+1.6}_{-1.4}$	$28.1^{+1.8\pm0.4}_{-1.5\pm0.2}$	$8.87^{+0.35}_{-0.28}$	$8.90^{+0.31}_{-0.27}$	$8.88^{+0.33\pm0.01}_{-0.28\pm0.04}$	$15.2^{+1.5}_{-1.1}$	$15.0^{+1.3}_{-1.0}$	$15.1^{+1.4\pm0.3}_{-1.1\pm0.0}$
Primary mass $m_1^\mathrm{source}/\mathrm{M}_\odot$	$37.0^{+4.9}_{-4.4}$	$35.3^{+5.1}_{-3.1}$	$36.2^{+5.2\pm1.4}_{-3.8\pm0.6}$	$14.0^{+10.0}_{-3.5}$	$14.5^{+6.6}_{-3.7}$	$14.2^{+8.3\pm1.4}_{-3.7\pm0.2}$	24^{+19}_{-7}	23^{+16}_{-5}	$23^{+18\pm4}_{-6\pm0}$
Secondary mass $m_2^\mathrm{source}/\mathrm{M}_\odot$	$28.3^{+4.6}_{-3.9}$	$29.9^{+3.0}_{-4.5}$	$29.1^{+3.7\pm0.7}_{-4.4\pm0.2}$	$7.5^{+2.3}_{-2.6}$	$7.4^{+2.3}_{-2.0}$	$7.5^{+2.3\pm0.2}_{-2.3\pm0.2}$	13^{+4}_{-5}	14^{+4}_{-5}	$13^{+4\pm0}_{-5\pm0}$
Final mass $M_\mathrm{f}^\mathrm{source}/\mathrm{M}_\odot$	$62.5^{+3.9}_{-3.5}$	$62.1^{+3.3}_{-2.8}$	$62.3^{+3.7\pm0.6}_{-3.1\pm0.3}$	$20.6^{+7.6}_{-1.6}$	$20.9^{+4.8}_{-1.8}$	$20.8^{+6.1\pm2.1}_{-1.7\pm0.2}$	36^{+15}_{-4}	35^{+11}_{-3}	$35^{+14\pm4}_{-4\pm0}$
Energy radiated $E_\mathrm{rad}/(\mathrm{M}_\odot c^2)$	$2.98^{+0.55}_{-0.40}$	$3.02^{+0.36}_{-0.36}$	$3.00^{+0.47\pm0.13}_{-0.39\pm0.07}$	$1.02^{+0.09}_{-0.24}$	$0.99^{+0.11}_{-0.17}$	$1.00^{+0.10\pm0.01}_{-0.20\pm0.03}$	$1.48^{+0.39}_{-0.41}$	$1.51^{+0.29}_{-0.44}$	$1.50^{+0.33\pm0.05}_{-0.43\pm0.01}$
Mass ratio q	$0.77^{+0.20}_{-0.18}$	$0.85^{+0.13}_{-0.21}$	$0.81^{+0.16\pm0.02}_{-0.20\pm0.04}$	$0.54^{+0.40}_{-0.33}$	$0.51^{+0.39}_{-0.25}$	$0.52^{+0.38\pm0.03}_{-0.29\pm0.04}$	$0.53^{+0.42}_{-0.34}$	$0.60^{+0.35}_{-0.37}$	$0.57^{+0.37\pm0.01}_{-0.37\pm0.04}$
Effective inspiral spin χ_eff	$-0.08^{+0.17}_{-0.14}$	$-0.05^{+0.11}_{-0.12}$	$-0.06^{+0.14\pm0.02}_{-0.14\pm0.04}$	$0.21^{+0.24}_{-0.11}$	$0.22^{+0.15}_{-0.08}$	$0.21^{+0.20\pm0.07}_{-0.10\pm0.03}$	$0.06^{+0.31}_{-0.24}$	$0.01^{+0.26}_{-0.17}$	$0.03^{+0.31\pm0.08}_{-0.20\pm0.02}$
Primary spin magnitude a_1	$0.33^{+0.39}_{-0.29}$	$0.30^{+0.54}_{-0.27}$	$0.32^{+0.47\pm0.10}_{-0.29\pm0.01}$	$0.42^{+0.35}_{-0.37}$	$0.55^{+0.35}_{-0.42}$	$0.49^{+0.37\pm0.11}_{-0.42\pm0.07}$	$0.31^{+0.46}_{-0.27}$	$0.31^{+0.50}_{-0.28}$	$0.31^{+0.48\pm0.03}_{-0.28\pm0.00}$
Secondary spin magnitude a_2	$0.62^{+0.35}_{-0.54}$	$0.36^{+0.53}_{-0.33}$	$0.48^{+0.47\pm0.08}_{-0.43\pm0.03}$	$0.51^{+0.44}_{-0.46}$	$0.52^{+0.42}_{-0.47}$	$0.52^{+0.43\pm0.01}_{-0.47\pm0.00}$	$0.49^{+0.45}_{-0.44}$	$0.42^{+0.50}_{-0.38}$	$0.45^{+0.48\pm0.02}_{-0.41\pm0.01}$
Final spin a_f	$0.68^{+0.05}_{-0.07}$	$0.68^{+0.06}_{-0.05}$	$0.68^{+0.05\pm0.01}_{-0.06\pm0.02}$	$0.73^{+0.05}_{-0.06}$	$0.75^{+0.07}_{-0.05}$	$0.74^{+0.06\pm0.03}_{-0.06\pm0.03}$	$0.65^{+0.09}_{-0.10}$	$0.66^{+0.08}_{-0.10}$	$0.66^{+0.09\pm0.00}_{-0.10\pm0.02}$
Luminosity distance $D_\mathrm{L}/\mathrm{Mpc}$	400^{+160}_{-180}	440^{+140}_{-170}	$420^{+150\pm20}_{-180\pm40}$	450^{+180}_{-210}	440^{+170}_{-180}	$440^{+180\pm20}_{-190\pm10}$	1000^{+540}_{-490}	1030^{+480}_{-480}	$1020^{+500\pm20}_{-490\pm40}$
Source redshift z	$0.086^{+0.031}_{-0.036}$	$0.094^{+0.027}_{-0.034}$	$0.090^{+0.029\pm0.003}_{-0.036\pm0.008}$	$0.096^{+0.035}_{-0.042}$	$0.092^{+0.033}_{-0.037}$	$0.094^{+0.035\pm0.004}_{-0.039\pm0.001}$	$0.198^{+0.091}_{-0.092}$	$0.204^{+0.082}_{-0.088}$	$0.201^{+0.086\pm0.003}_{-0.091\pm0.008}$
Upper bound									
Primary spin magnitude a_1	0.62	0.73	0.67 ± 0.09	0.68	0.83	0.77 ± 0.12	0.64	0.69	0.67 ± 0.04
Secondary spin magnitude a_2	0.93	0.80	0.90 ± 0.12	0.90	0.89	0.90 ± 0.01	0.89	0.85	0.87 ± 0.04
Lower bound									
Mass ratio q	0.62	0.68	0.65 ± 0.05	0.25	0.30	0.28 ± 0.04	0.22	0.28	0.24 ± 0.05
Log Bayes factor $\ln \mathscr{B}_{s/n}$	287.7 ± 0.1	289.8 ± 0.3	—	59.5 ± 0.1	60.2 ± 0.2	—	22.8 ± 0.2	23.0 ± 0.1	—
Information criterion DIC	32977.2 ± 0.3	32973.1 ± 0.1	—	34296.4 ± 0.2	34295.1 ± 0.1	—	94695.8 ± 0.0	94692.9 ± 0.0	—

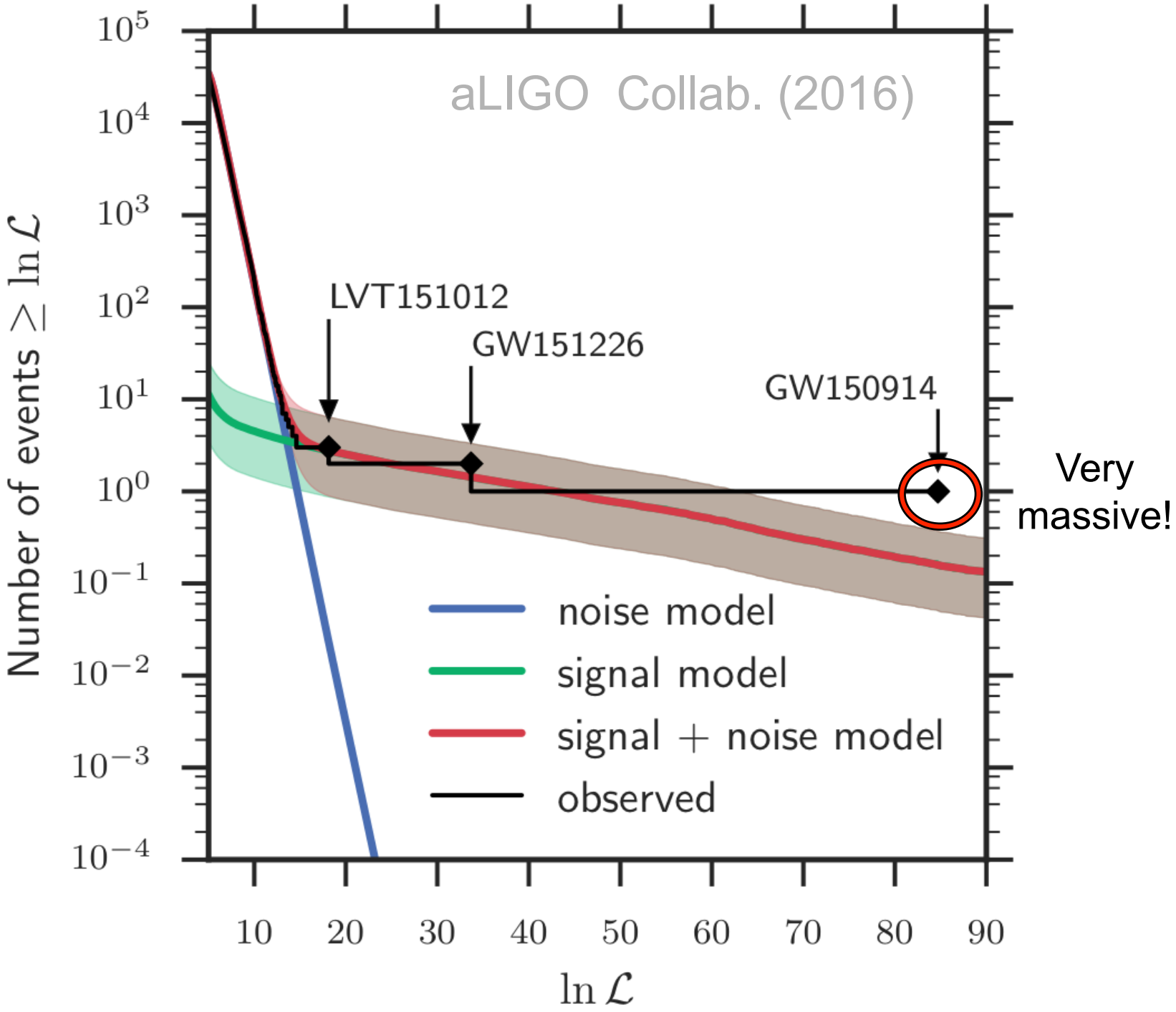
aLIGO Collab. (2016)
LVT151012
GW151226
GW150914
Very massive!
noise model
signal model
signal + noise model
observed
Number of events $\geq \ln \mathcal{L}$
$\ln \mathcal{L}$
10^5
10^4
10^3
10^2
10^1
10^0
10^{-1}
10^{-2}
10^{-3}
10^{-4}
10
20
30
40
50
60
70
80
90

Mass distribution	$R/(\mathrm{Gpc}^{-3}\mathrm{yr}^{-1})$		
	PyCBC	GstLAL	Combined
	Event based		
GW150914	$3.2^{+8.3}_{-2.7}$	$3.6^{+9.1}_{-3.0}$	$3.4^{+8.6}_{-2.8}$
LVT151012	$9.2^{+30.3}_{-8.5}$	$9.2^{+31.4}_{-8.5}$	$9.4^{+30.4}_{-8.7}$
GW151226	35^{+92}_{-29}	37^{+94}_{-31}	37^{+92}_{-31}
All	53^{+100}_{-40}	56^{+105}_{-42}	55^{+99}_{-41}
	Astrophysical		
Flat in log mass	31^{+43}_{-21}	30^{+43}_{-21}	30^{+43}_{-21}
Power Law (-2.35)	100^{+136}_{-69}	95^{+138}_{-67}	99^{+138}_{-70}

TABLE II. Rates of BBH mergers based on populations with masses matching the observed events, and astrophysically motivated mass distributions. Rates inferred from the PyCBC and GstLAL analyses independently as well as combined rates are shown. The table shows median values with 90% credible intervals.

Gravitational Wave Astronomy

- Discovery of binary BH by aLIGO
- VIRGO, KAGRA, INDIGO = GW Astron
- GW150914 = 36 + 29 M_{sun} BH binary
- GW151226 = 14 + 8 M_{sun} BH binary
- LVT151012 = 23 + 13 M_{sun} “candidate”
- Expected 50-100 events/yr/Gpc^3
- aLIGO+ can map the mass and spin of Massive BH (10 M_{sun} < M_{BH} < 150 M_{sun})

Massive Primordial Black Holes as DM

PHYSICAL REVIEW D VOLUME 54, NUMBER 10 15 NOVEMBER 1996

Density perturbations and black hole formation in hybrid inflation

Juan García-Bellido
Astronomy Centre, University of Sussex, Falmer, Brighton BN1 9QH, United Kingdom

. The resulting density inhomogeneities lead to a copious production of black holes.

David Wands
School of Mathematical Studies, University of Portsmouth, Portsmouth PO1 2EG, United Kingdom
and Astronomy Centre, University of Sussex, Falmer, Brighton BN1 9QH, United Kingdom

for certain values of parameters these black holes may constitute the dark matter in the Universe.

corresponding to the phase transition. The resulting density inhomogeneities lead to a copious production of black holes. This could be an argument against hybrid inflation models with two stages of inflation. However, we find a class of models where this problem can be easily avoided. The number of black holes produced in these models can be made extremely small, but in general it could be sufficiently large to have important cosmological and astrophysical implications. In particular, for certain values of parameters these black holes may constitute the dark matter in the Universe. It is also possible to have hybrid models with two stages of inflation where the black hole production is not suppressed, but where the typical masses of the black holes are very small. Such models lead to a completely different thermal history of the Universe, where postinflationary reheating occurs via black hole evaporation. [S0556-2821(96)00522-X]

PACS number(s): 98.80.Cq

Steven Weinberg

“our problem is not that we
take our theories too seriously,
but that we
don't take them seriously enough”

PHYSICAL REVIEW D 92, 023524 (2015)

Massive primordial black holes from hybrid inflation as dark matter

These PBHs could have acquired large stellar masses today, via merging, the model passes both the constraints from CMB distortions and microlensing. the tail of the PBH mass distribution could be responsible for the seeds of supermassive black holes at the center of galaxies, as well as for ultraluminous x-ray sources.

matter today, while the matter power spectrum on scales probed by cosmic microwave background (CMB) anisotropies agrees with Planck data. These PBHs could have acquired large stellar masses today, via merging, and the model passes both the constraints from CMB distortions and microlensing. This scenario is supported by Chandra observations of numerous BH candidates in the central region of Andromeda. Moreover, the tail of the PBH mass distribution could be responsible for the seeds of supermassive black holes at the center of galaxies, as well as for ultraluminous x-ray sources. We find that our effective hybrid potential can originate e.g. from D-term inflation with a Fayet-Iliopoulos term of the order of the Planck scale but sub-Planckian values of the inflaton field. Finally, we discuss the implications of quantum diffusion at the instability point of the potential, able to generate a Swiss-cheese-like structure of the Universe, eventually leading to apparent accelerated cosmic expansion.

DOI: 10.1103/PhysRevD.92.023524 PACS numbers: 98.80.Cq

Moreover, PBH binaries should emit gravitational waves that could be detected by future gravitational wave experiments such as LIGO, DECIGO and eLISA [70,71].

Binaries of PBHs forming a fraction of dark matter should emit gravitational waves; this results in a background of gravitational waves that could be observed by LIGO, DECIGO and eLISA [70–72].

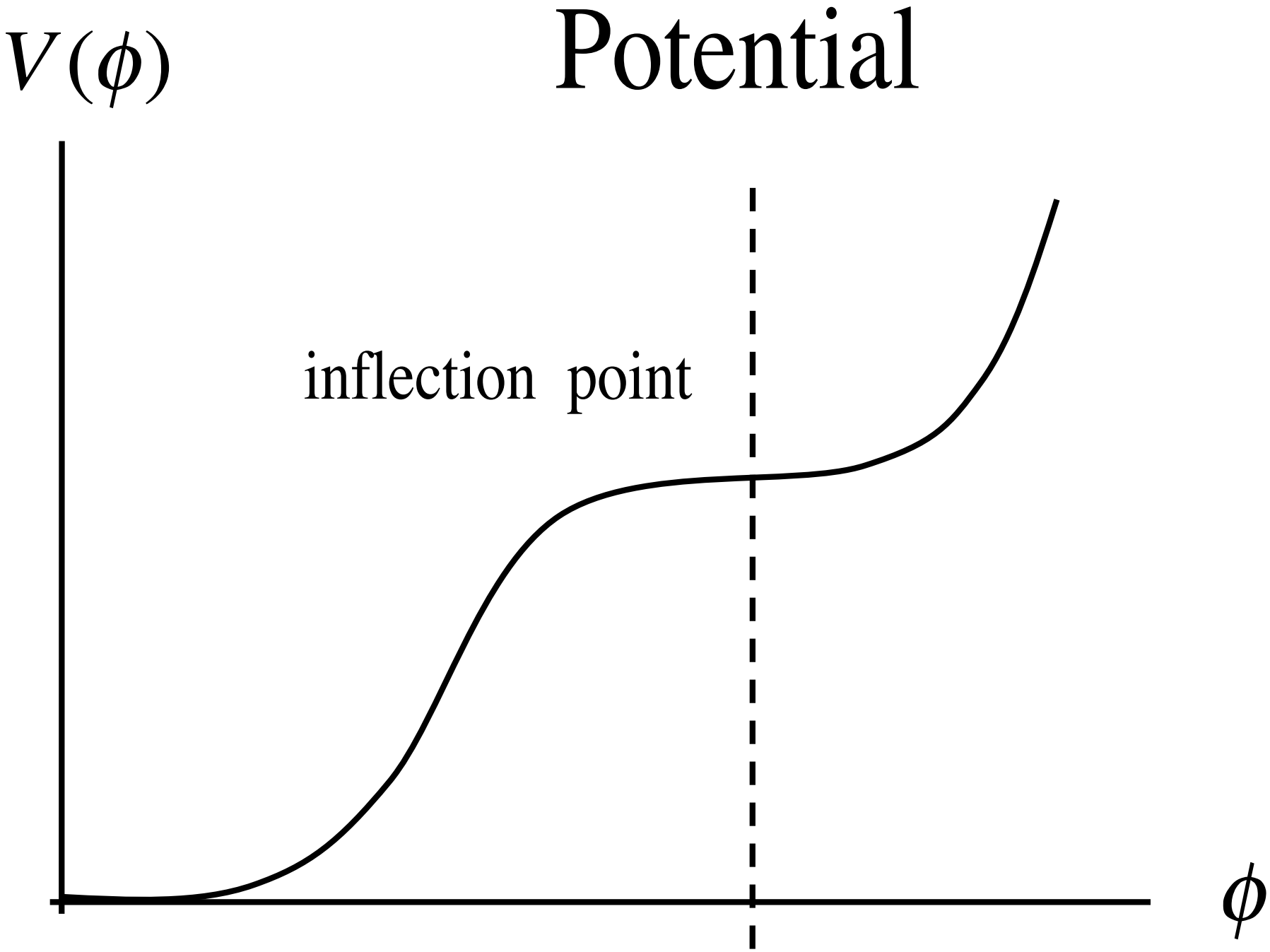
$V(\phi)$
Potential
inflection point
ϕ

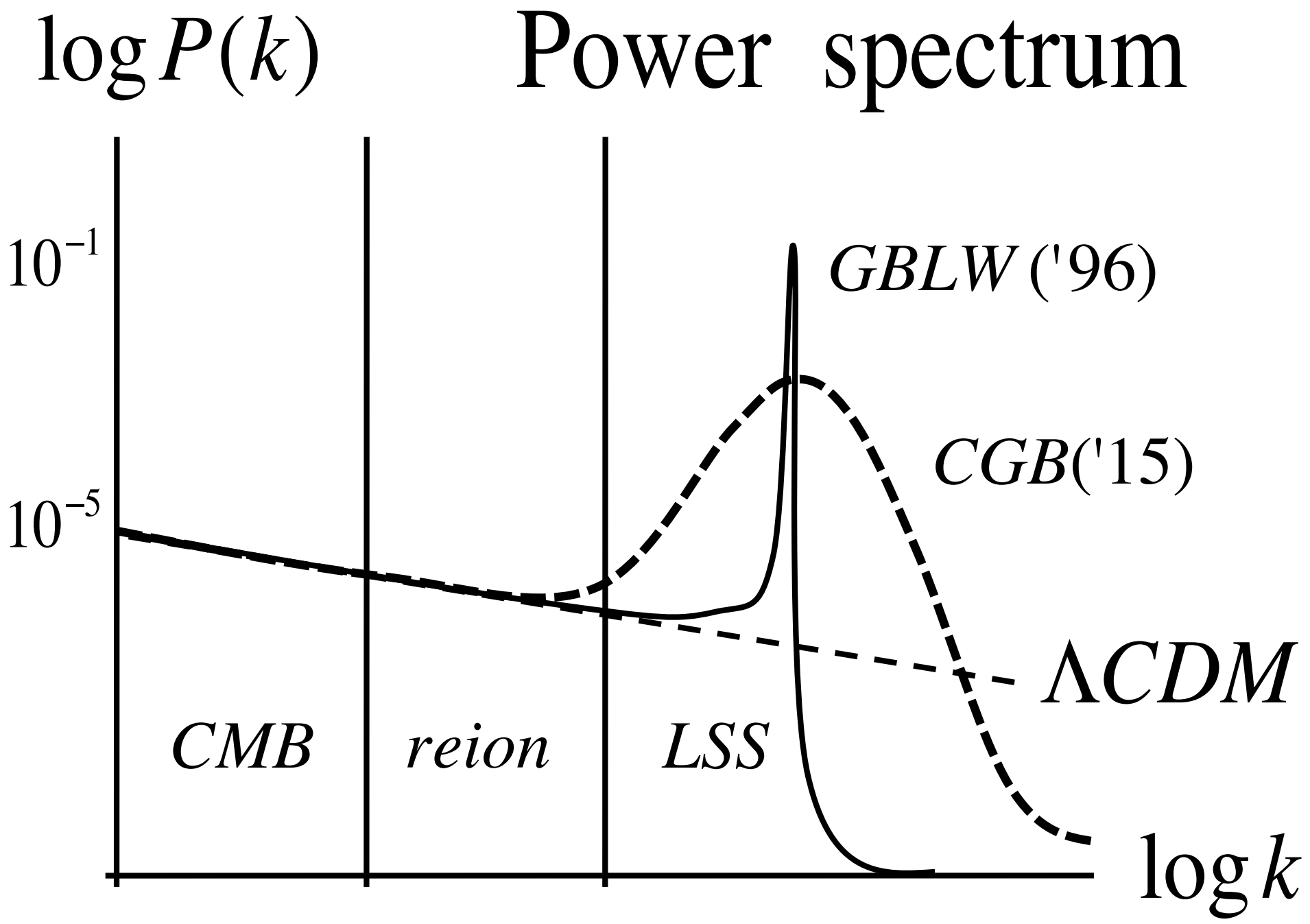
log P(k)
Power spectrum
10^-1
10^-5
GBLW ('96)
CGB('15)
ΛCDM
CMB
reion
LSS
log k

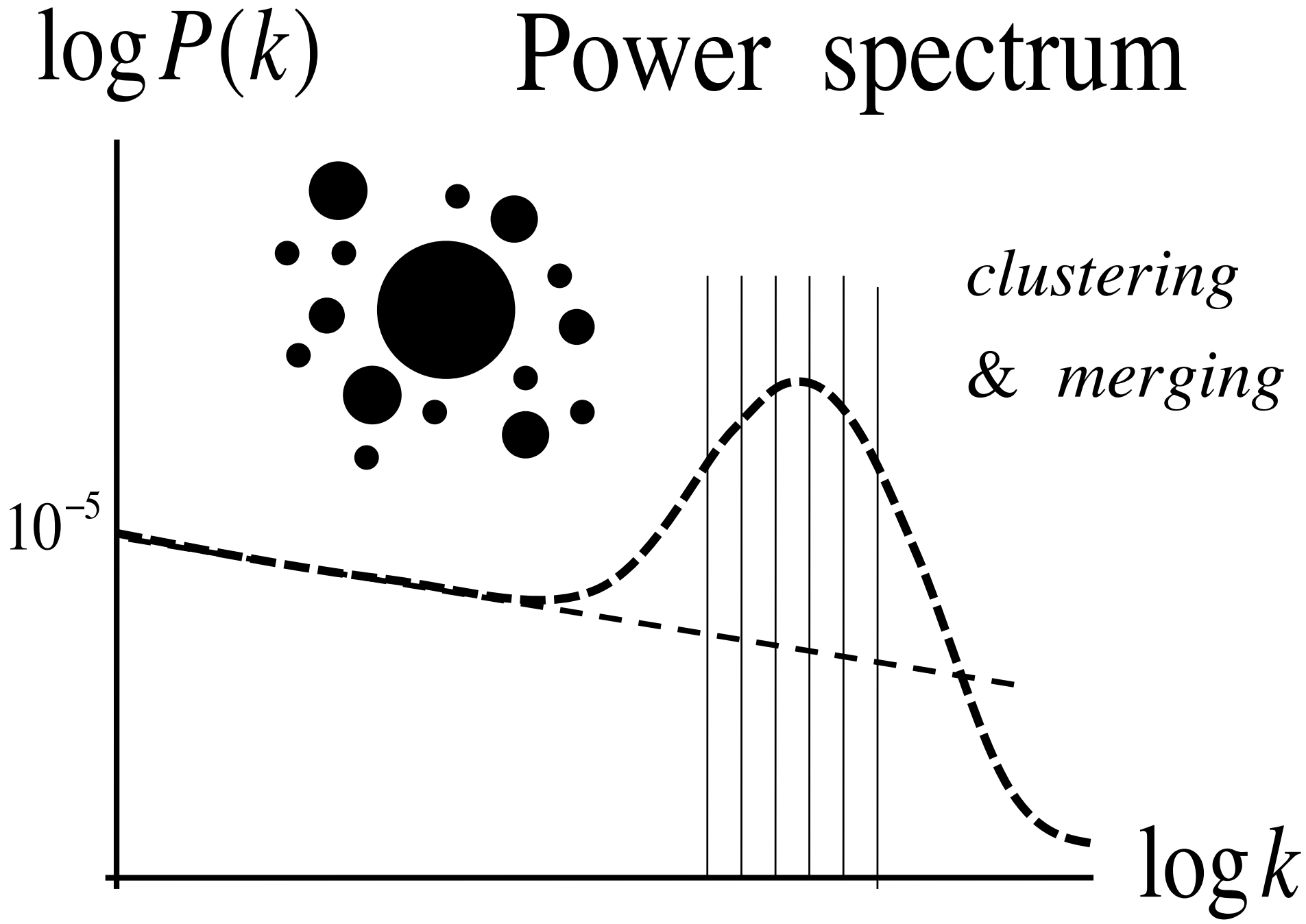
log P(k)
Power spectrum
clustering
& merging
10^−5
log k

Mass Spectrum @ formation during radiation era

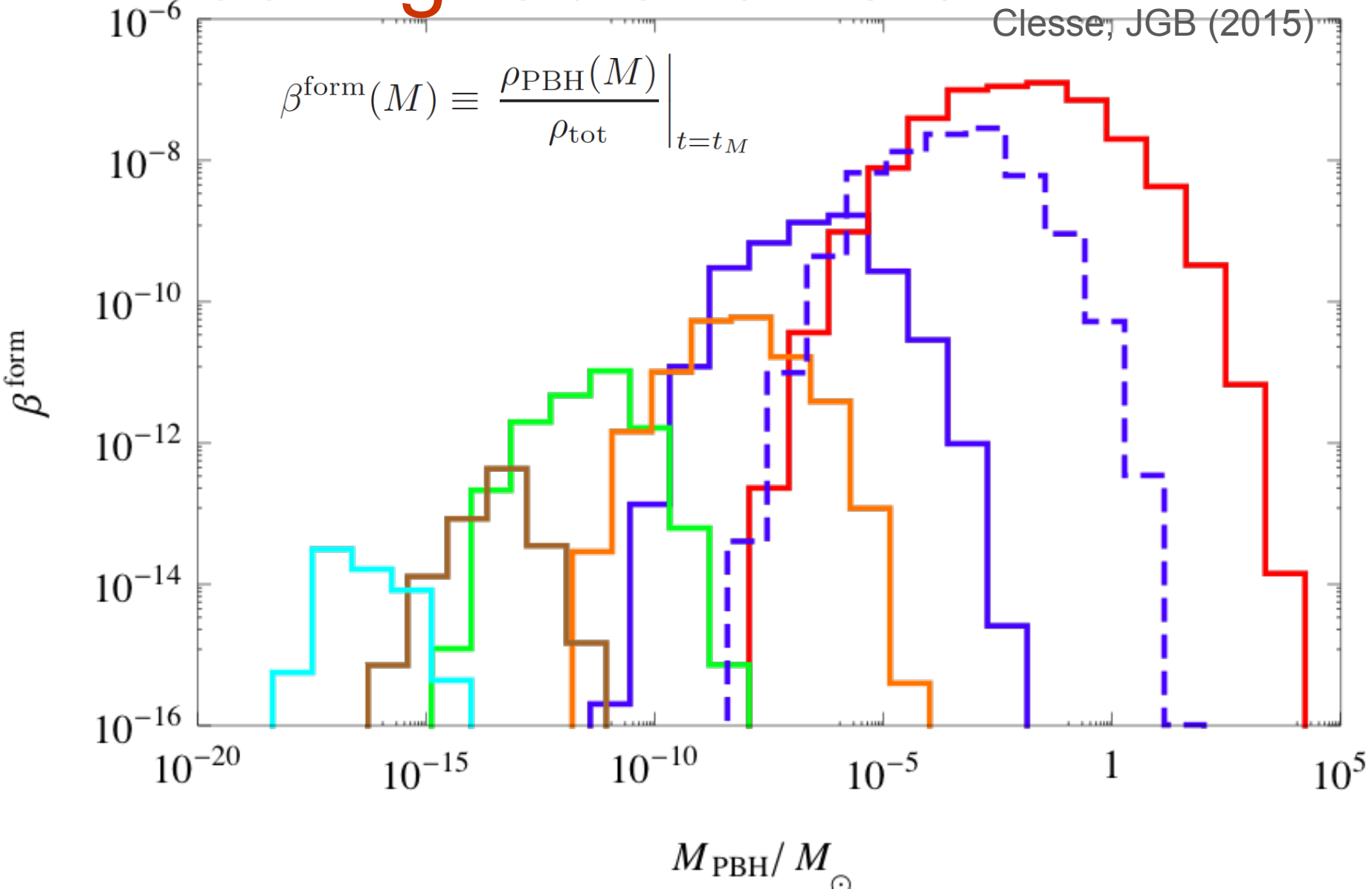

Mass Spectrum @ MR equality

Clesse, JGB (2015)

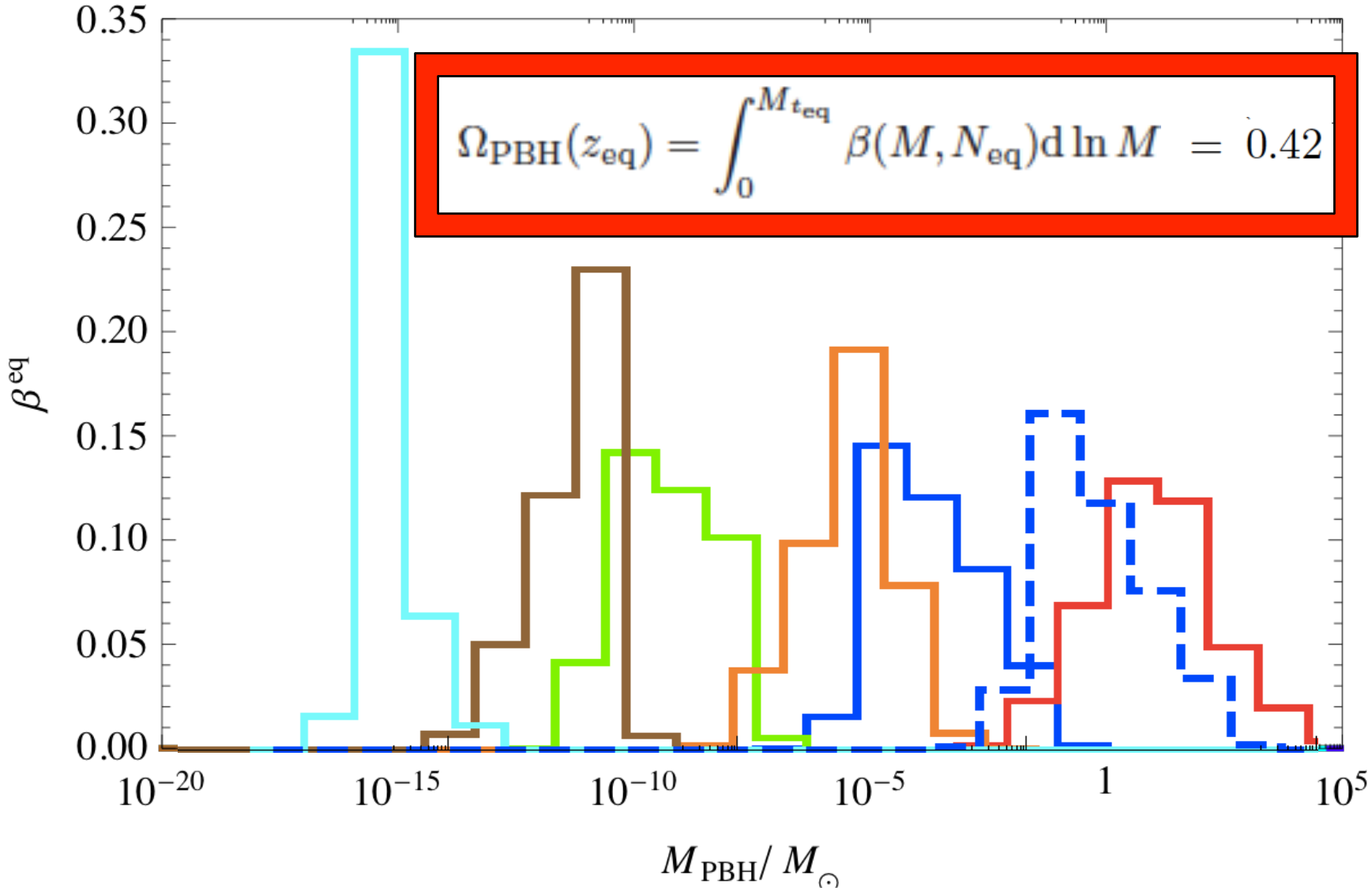

Constraints on Primordial Black Holes

Present Constraints on PBH

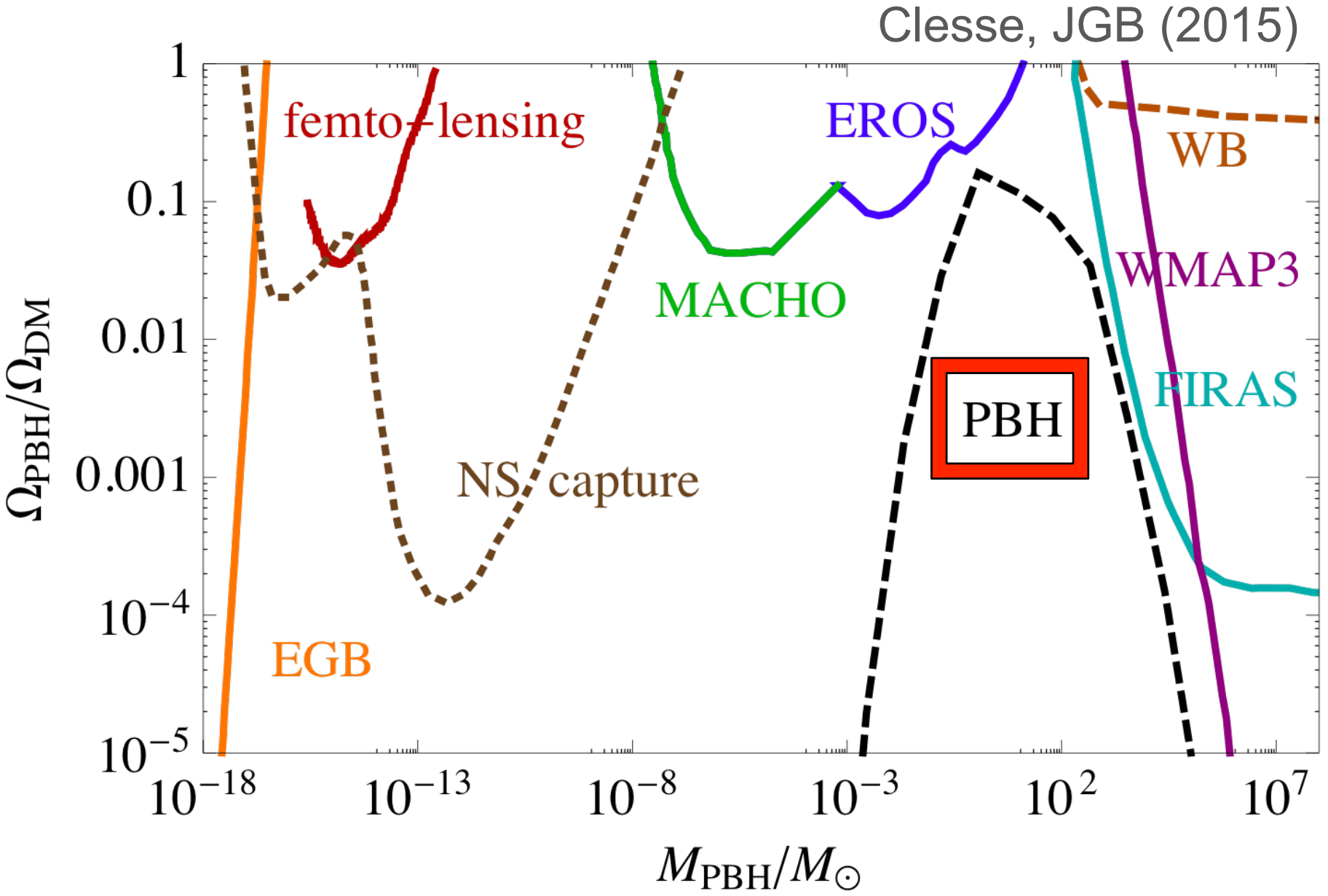

Massive Primordial Black Holes

- These are NOT the (small) PBH with $10^{-24}\ M_\odot < M_{PBH} < 10^{-6}\ M_\odot$ of Carr et al.
- These are MASSIVE black holes with $10^{-2}\ M_\odot < M_{PBH} < 10^{5}\ M_\odot$ which cluster and merge and could resolve some of the most acute problems of ΛCDM paradigm.
- ΛCDM N-body simulations never reach the $100\ M_\odot$ particle resolution, so for them PBH is as good as PDM.

Mass distribution of BH

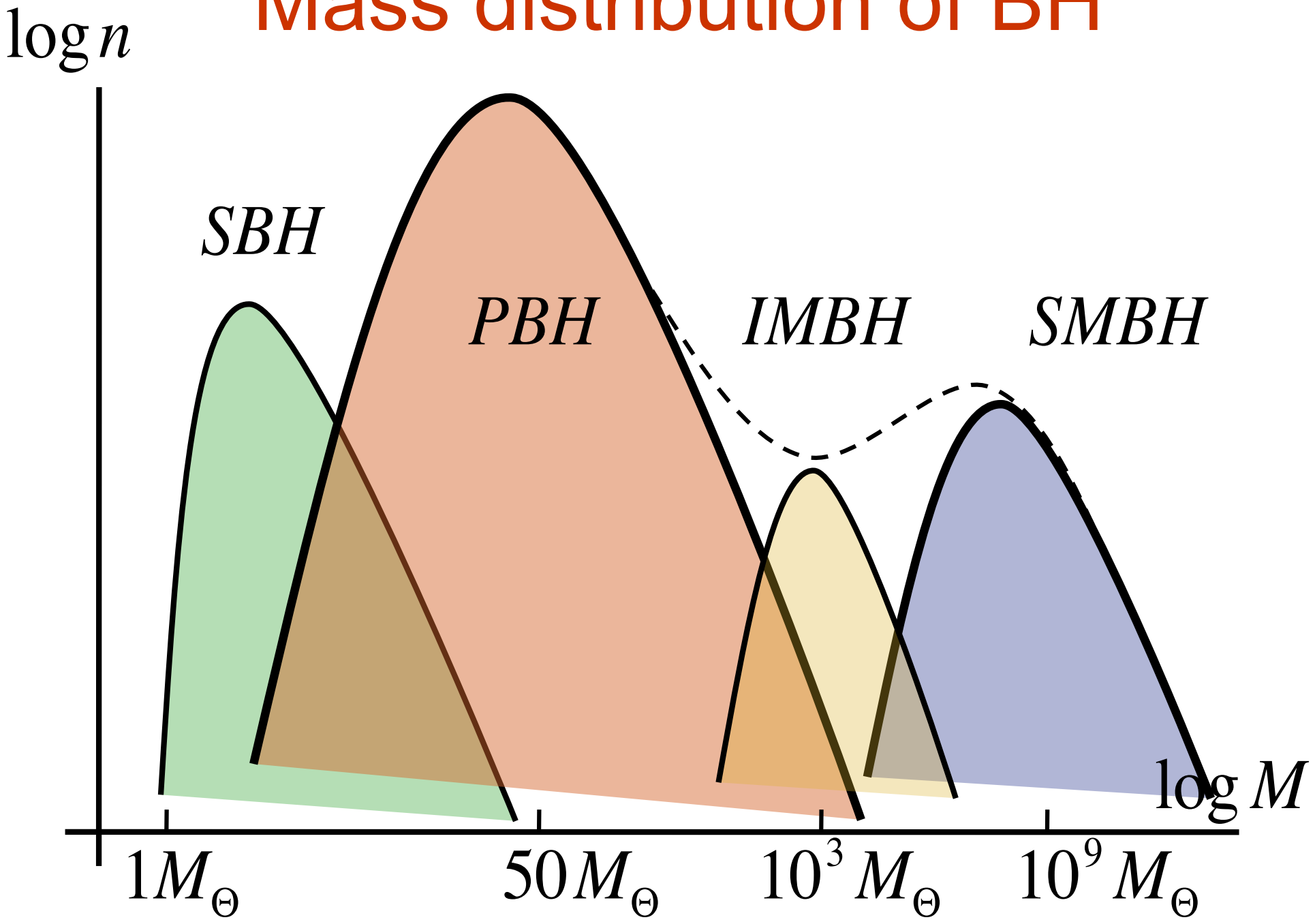

Mass-σ relation BH at G.C.

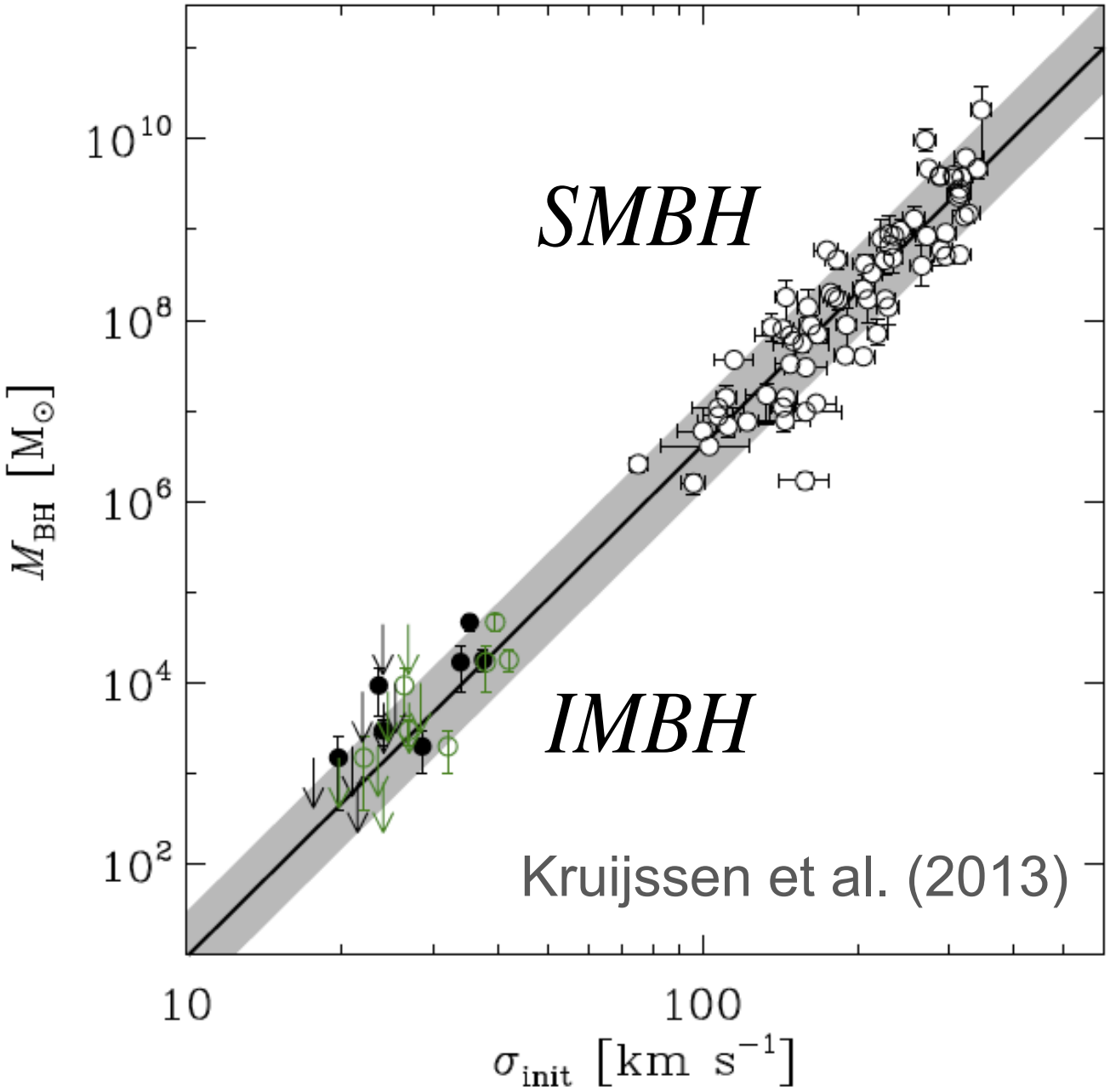

Distinguish MPBH from Stellar BH

- Accretion disks
- Distribution of spins
- Mass distribution ≠ IMF
- SBH kicks at formation vs static PBH
- Galaxy formation rate ➔ gal. seeds
- Microlensing events of long duration
- GAIA anomalous astrometry
- CMB distortions with PIXIE/PRISM
- Reionization faster in the past
- N-body simulations below 10^2 M_{sun}

Signatures of Primordial Black Holes

Microlensing

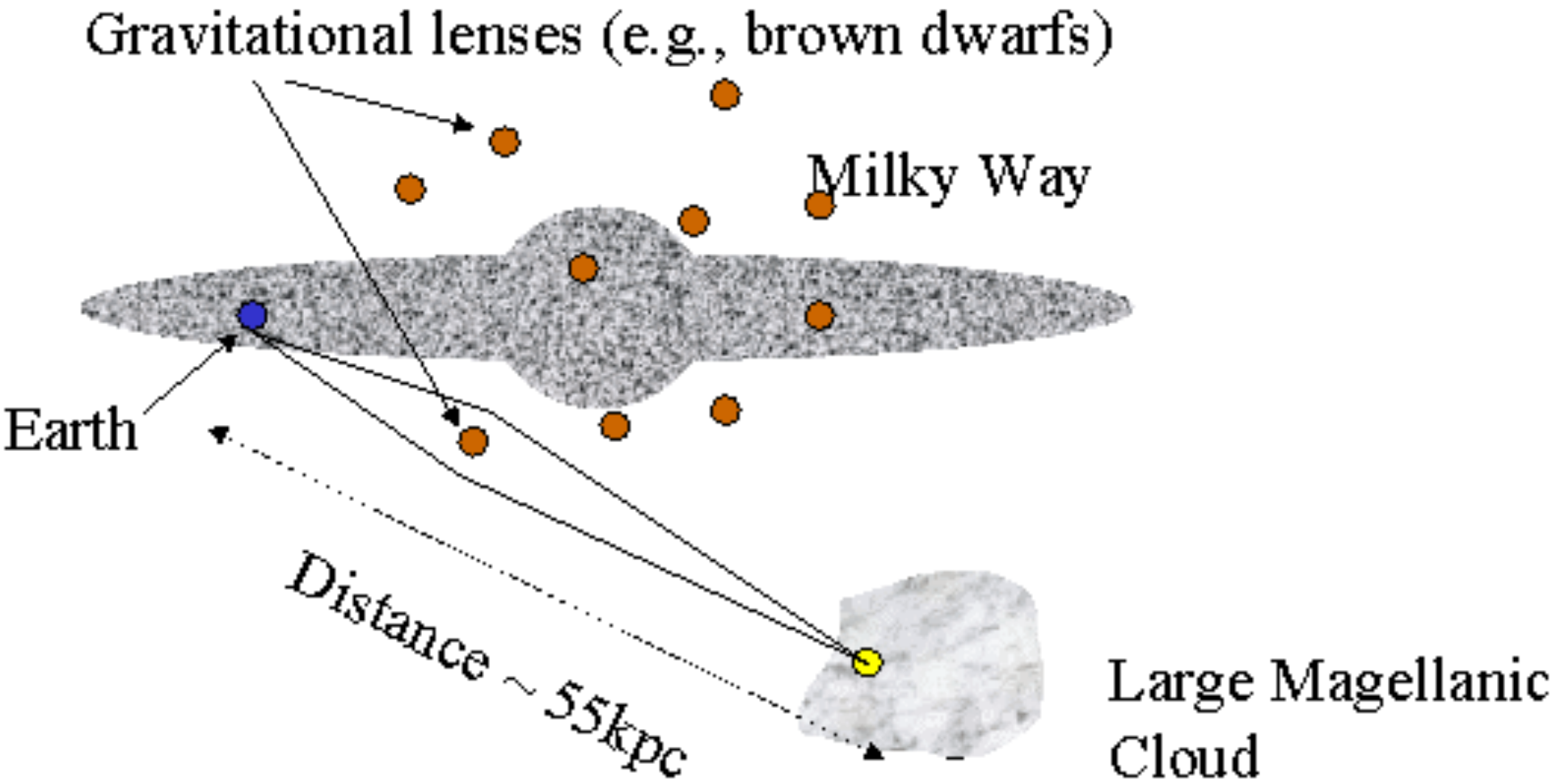

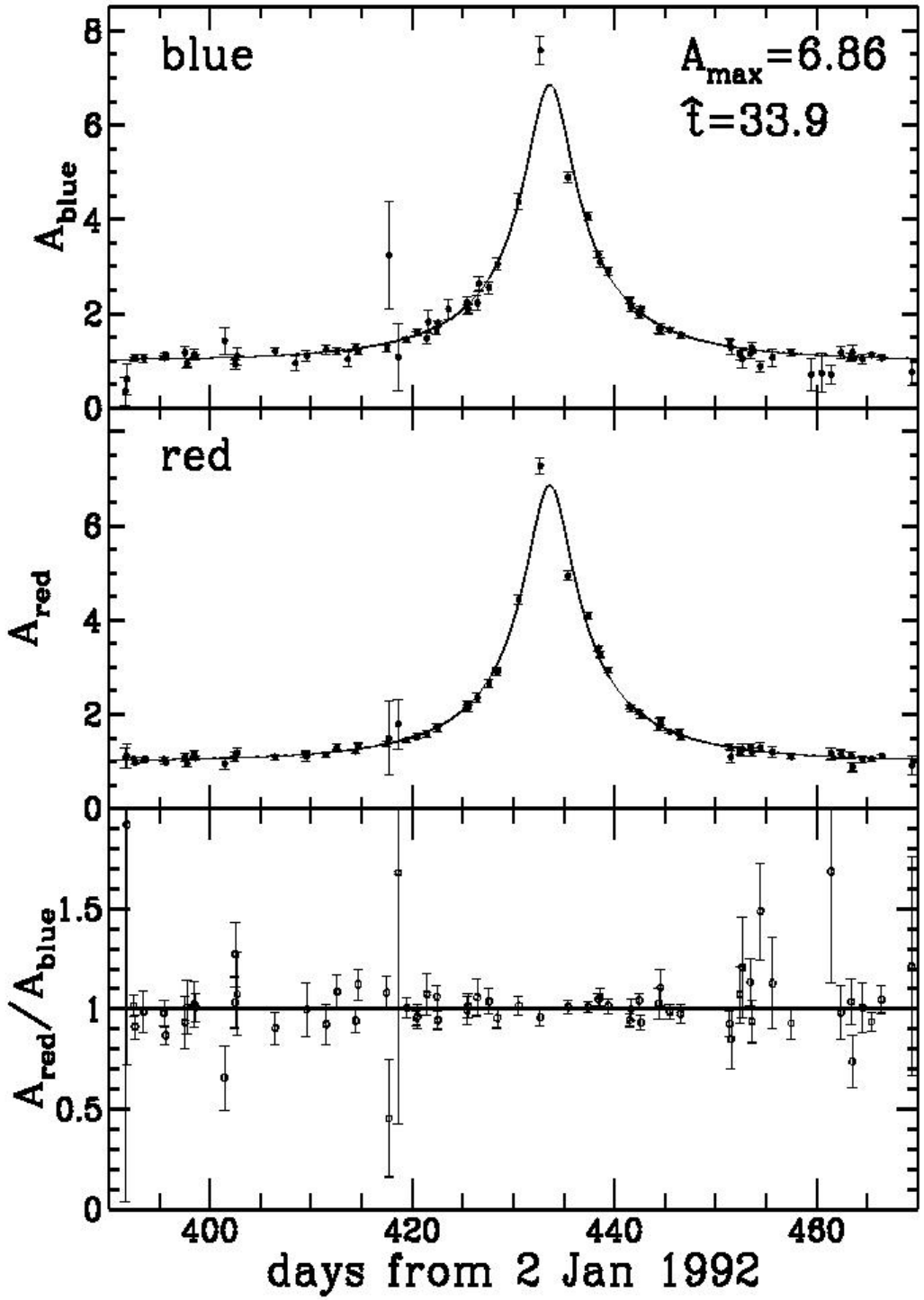

symmetric

$$A_{max} = 7.20 \pm 0.09$$

achromatic

$$\frac{A_{red}}{A_{blue}} = 1.00 \pm 0.05$$

unique

$$t = 34.8 \pm 0.2 \text{ days}$$

$$\Rightarrow \quad M_D \approx 0.1 M_\Theta$$

$$A = \frac{2+u^2}{u\sqrt{4+u^2}} \qquad u = \frac{r}{r_E} \quad \text{amplification}$$

$$\overline{\Delta t} = \frac{r_E}{\upsilon} = \frac{\sqrt{4GM_D d}}{\upsilon} \quad \text{average } \frac{1}{2} \text{ crossing}$$

$$M_D = 10\ M_\Theta \quad \Rightarrow \quad \overline{\Delta t} = 1.23 \text{ years}$$

$$M_D = 1\ M_\Theta \quad \Rightarrow \quad \overline{\Delta t} = 5 \text{ months}$$

$$M_D = 0.1\ M_\Theta \quad \Rightarrow \quad \overline{\Delta t} = 1.5 \text{ months}$$

$$M_D = 10^{-2}\ M_\Theta \quad \Rightarrow \quad \overline{\Delta t} = 2 \text{ weeks}$$

$$M_D = 10^{-4}\ M_\Theta \quad \Rightarrow \quad \overline{\Delta t} = 1.5 \text{ day}$$

P. Tisserand (2007)

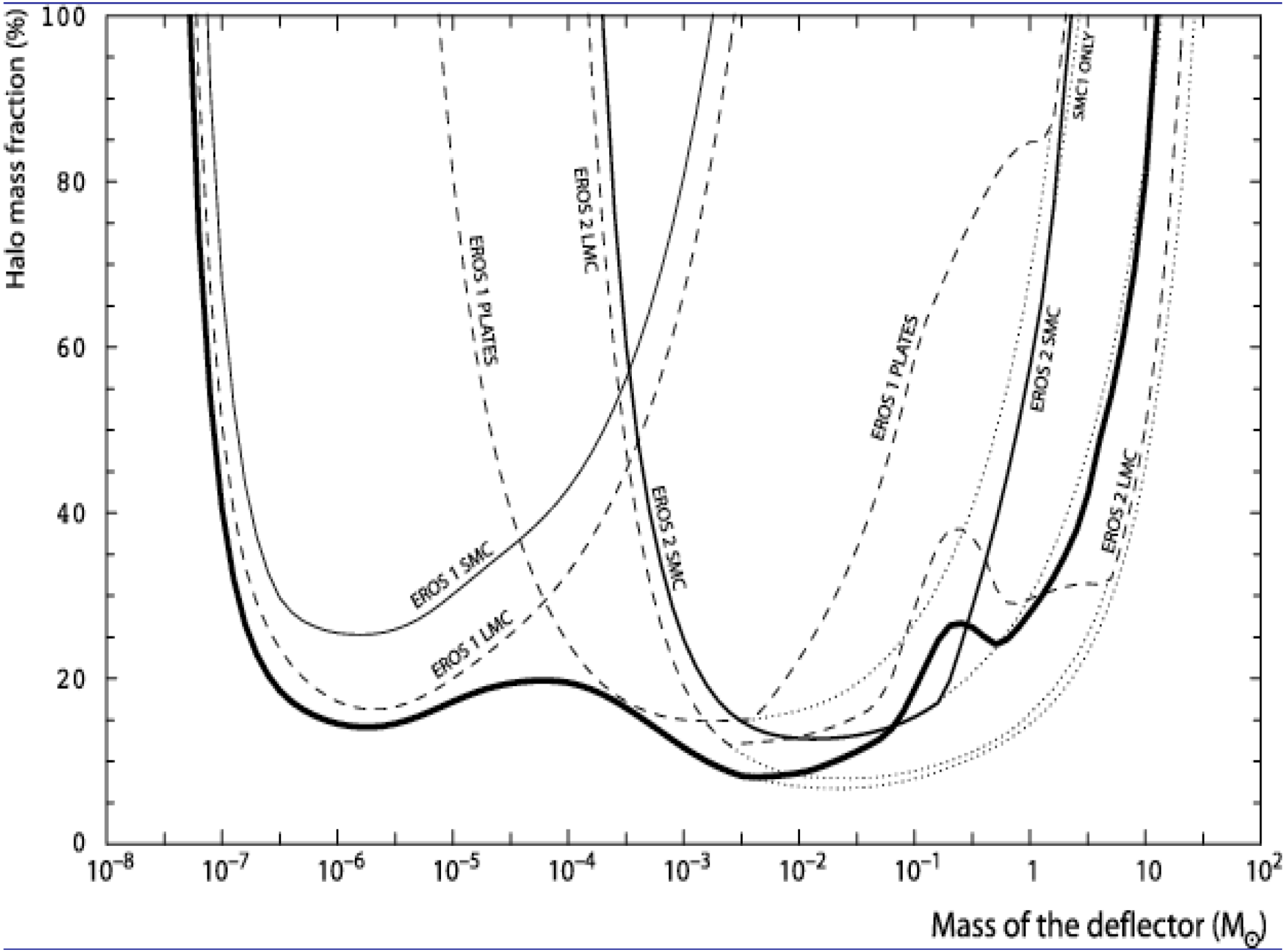

Astrometric Anomalies @ GAIA

GAIA position + velocity anomalies

Thomson model

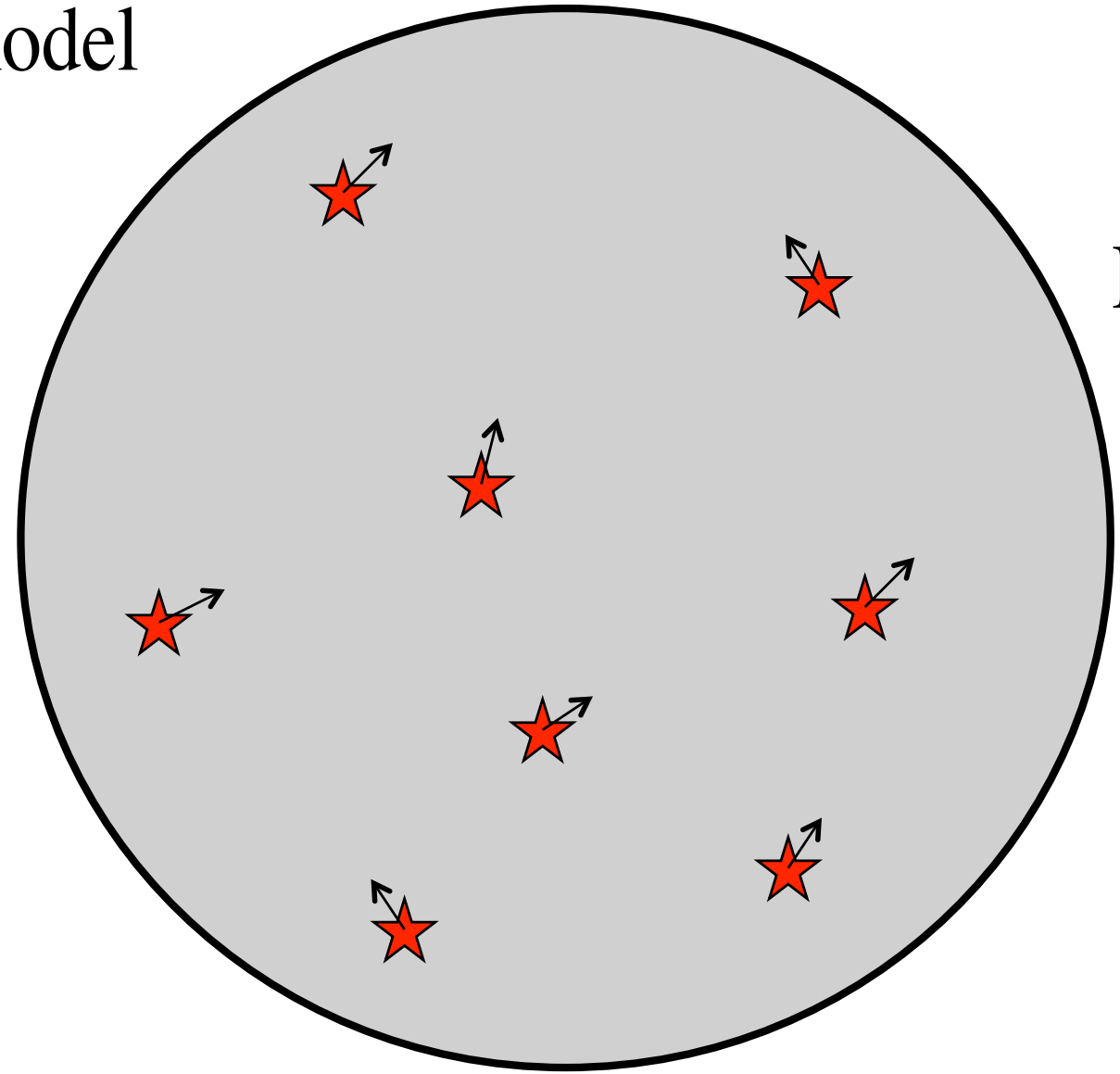

PDM

GAIA position + velocity anomalies

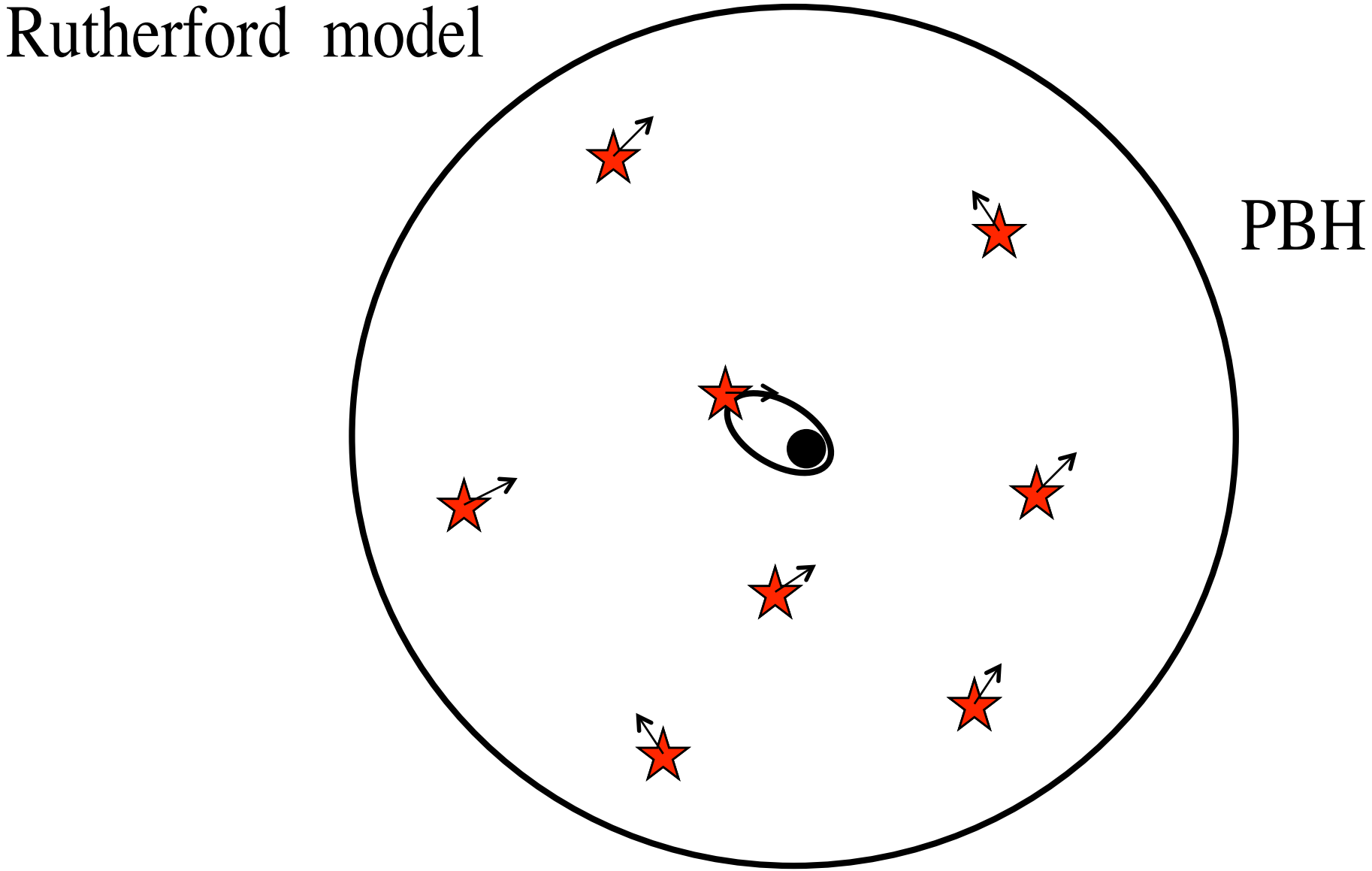

Average distance between PBH

$$M_{halo\,MW}(<50kpc) = 5.4\times10^{11}\,M_{\Theta}$$

$$\overline{\lambda}_{BH} \equiv (\overline{n}_{BH})^{-1/3} = 20\ \mathrm{pc}\left(\frac{M}{50\,M_{\Theta}}\right)^{1/3}$$

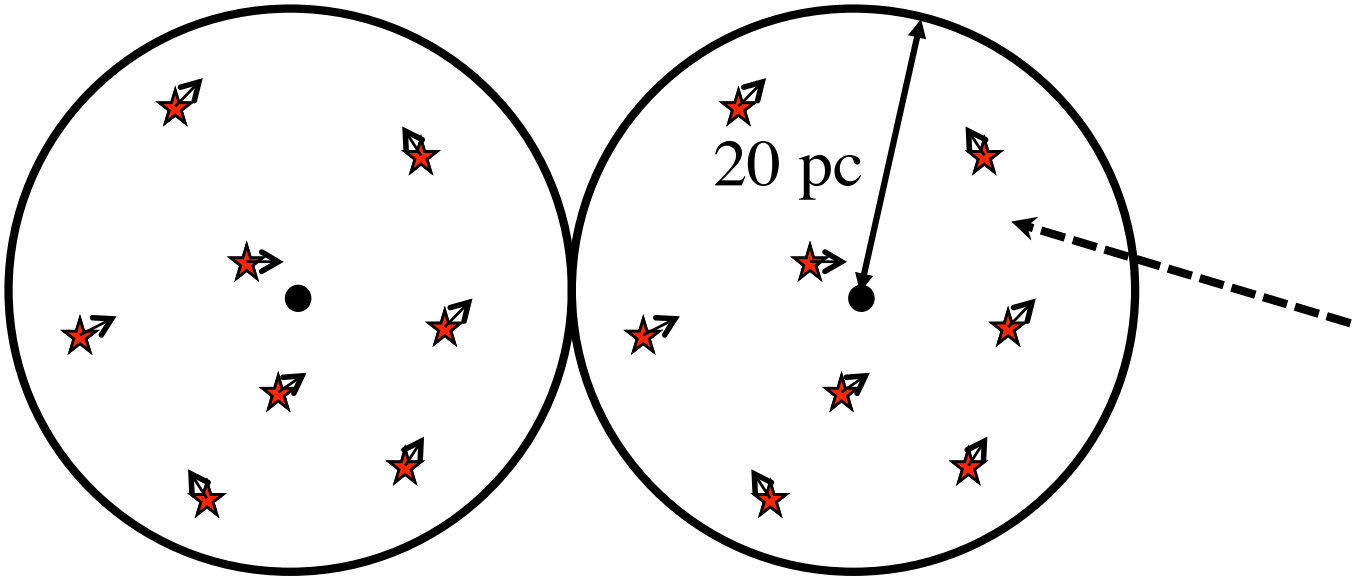

55000 stars per black hole of 50 M_{Θ} in our (solar) neighbourhood

Anomalous accelerations

The acceleration on any given star is due to the surrounding masses. A uniform DM field does not induce an extra force on ★. The ★ only feels the presence of other ★s

$$a_i = \frac{GM_{BH}}{b^2} + \sum_j \frac{Gm_j}{r_{ij}^2}\hat{u}_{ij}$$

$$\Delta a = \frac{GM_{BH}}{b^2} = 1\times 10^{-15}\, ms^{-2}\left(\frac{M}{50\,M_\Theta}\right)\left(\frac{20\,pc}{b}\right)^2$$

Anomalous velocities & positions

The relative velocity change of a ★ due to PBH, for a 220 km/s relative motion is

$$\frac{\Delta v}{v} = 3\times 10^{-4}\left(\frac{M}{50 M_{\odot}}\right)\left(\frac{0.1 pc}{b}\right)^{2}$$

The relative displacement of a ★ at 1 kpc

$$\frac{\Delta x}{x} = 0.56\ \text{marcsec}\left(\frac{M}{50 M_{\odot}}\right)\left(\frac{0.1 pc}{b}\right)^{2}$$

Gravitational slingshot effect

Close encounters of a star with MPBH @ 100 km/s relative motion is enough to expel the star from the globular cluster.

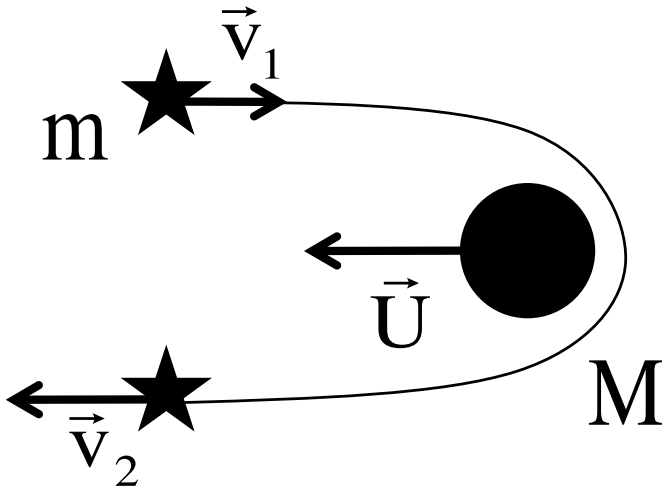

$$\vec{v}_2 = \frac{2\vec{U} + (1 - m/M)\vec{v}_1}{(1 + m/M)}$$

It may explain large M/L ratios of dSph by ejection of stars in the cluster, $v > v_{esc}$.

Fluctuations CIB & X-ray Background

Kashlinsky (2016)

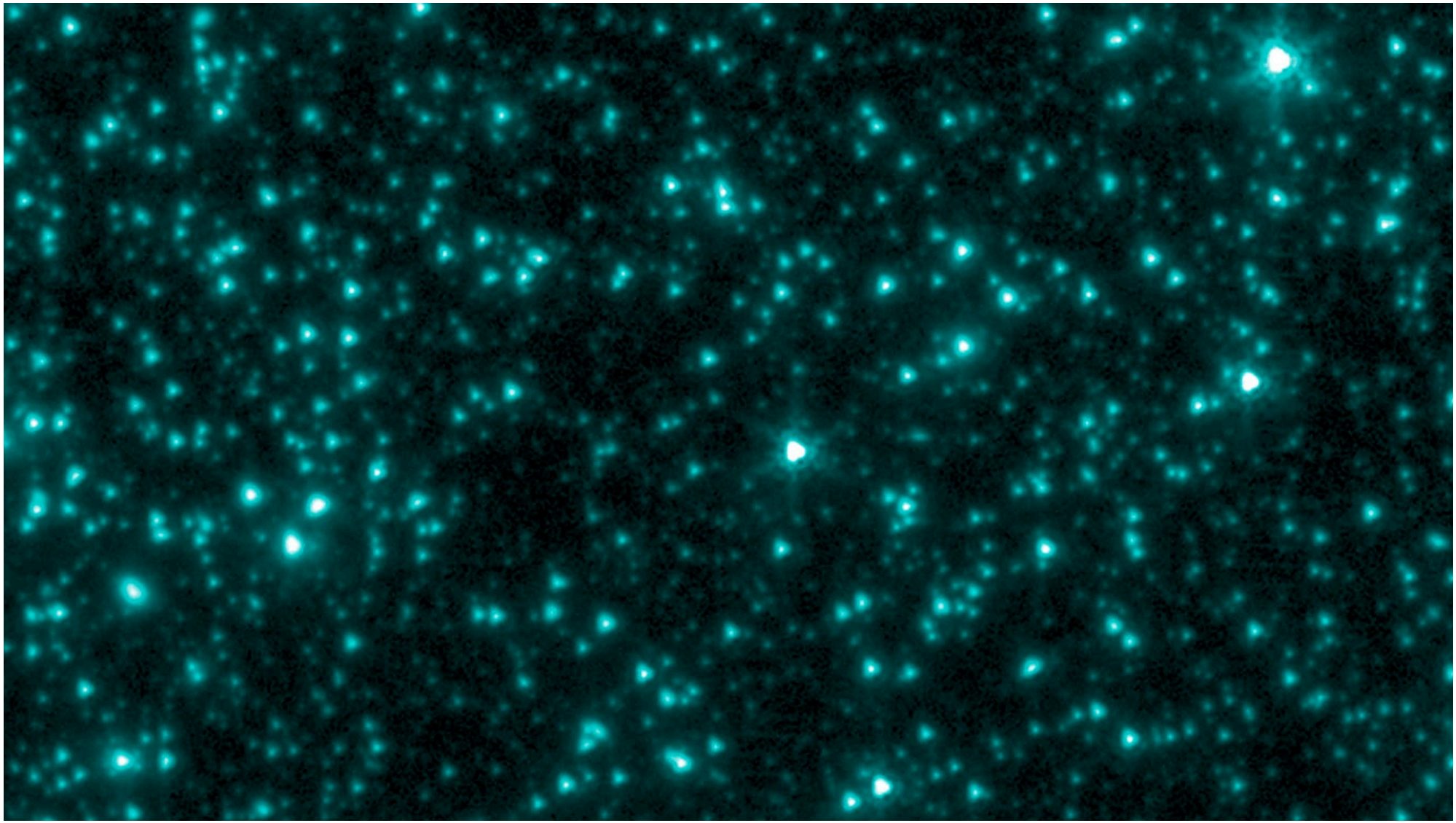

Kashlinsky (2016)

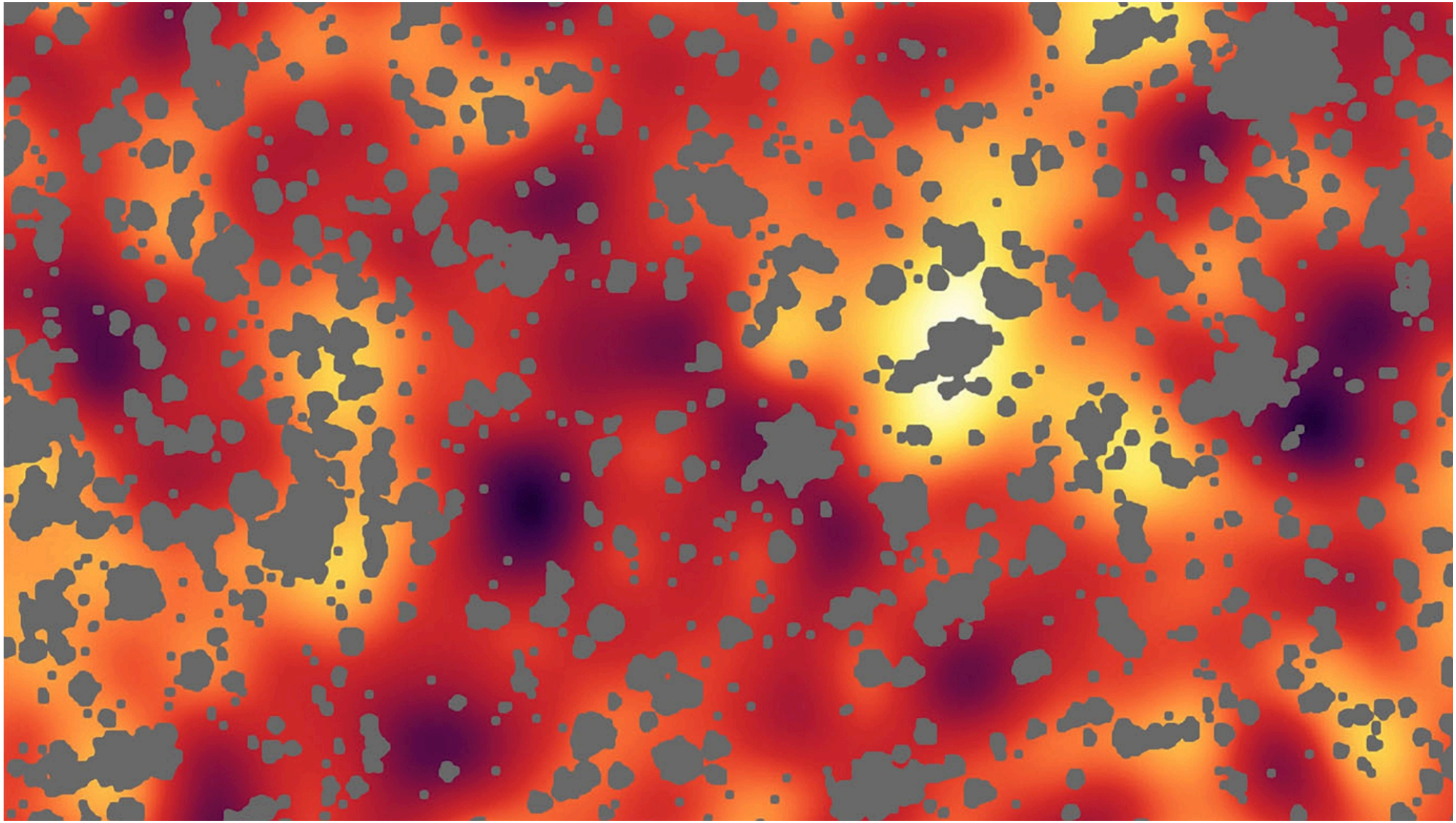

Grav. Waves detections @ aLIGO

The clustering of massive Primordial Black Holes as Dark Matter: measuring their mass distribution with Advanced LIGO

Sébastien Clesse[1,*] and Juan García-Bellido[2,†]

[1] *Institute for Theoretical Particle Physics and Cosmology (TTK), RWTH Aachen University, D-52056 Aachen, Germany*

[2] *Instituto de Física Teórica UAM-CSIC, Universidad Autonóma de Madrid, Cantoblanco, 28049 Madrid, Spain*

(Dated: March 17, 2016)

The recent detection by Advanced LIGO of gravitational waves (GW) from the merging of a binary black hole system sets new limits on the merging rates of massive primordial black holes (PBH) that could be a significant fraction or even the totality of the dark matter in the Universe. aLIGO opens the way to the determination of the distribution and clustering of such massive PBH. If PBH clusters have a similar density to the one observed in ultra-faint dwarf galaxies, we find merging rates comparable to aLIGO expectations. Massive PBH dark matter predicts the existence of thousands of those dwarf galaxies where star formation is unlikely because of gas accretion onto PBH, which would possibly provide a solution to the missing satellite and too-big-to-fail problems. Finally, we study the possibility of using aLIGO and future GW antennas to measure the abundance and mass distribution of PBH in the range [5 - 200] $M_\odot$ to 10% accuracy.

PACS numbers: 98.80.Cq

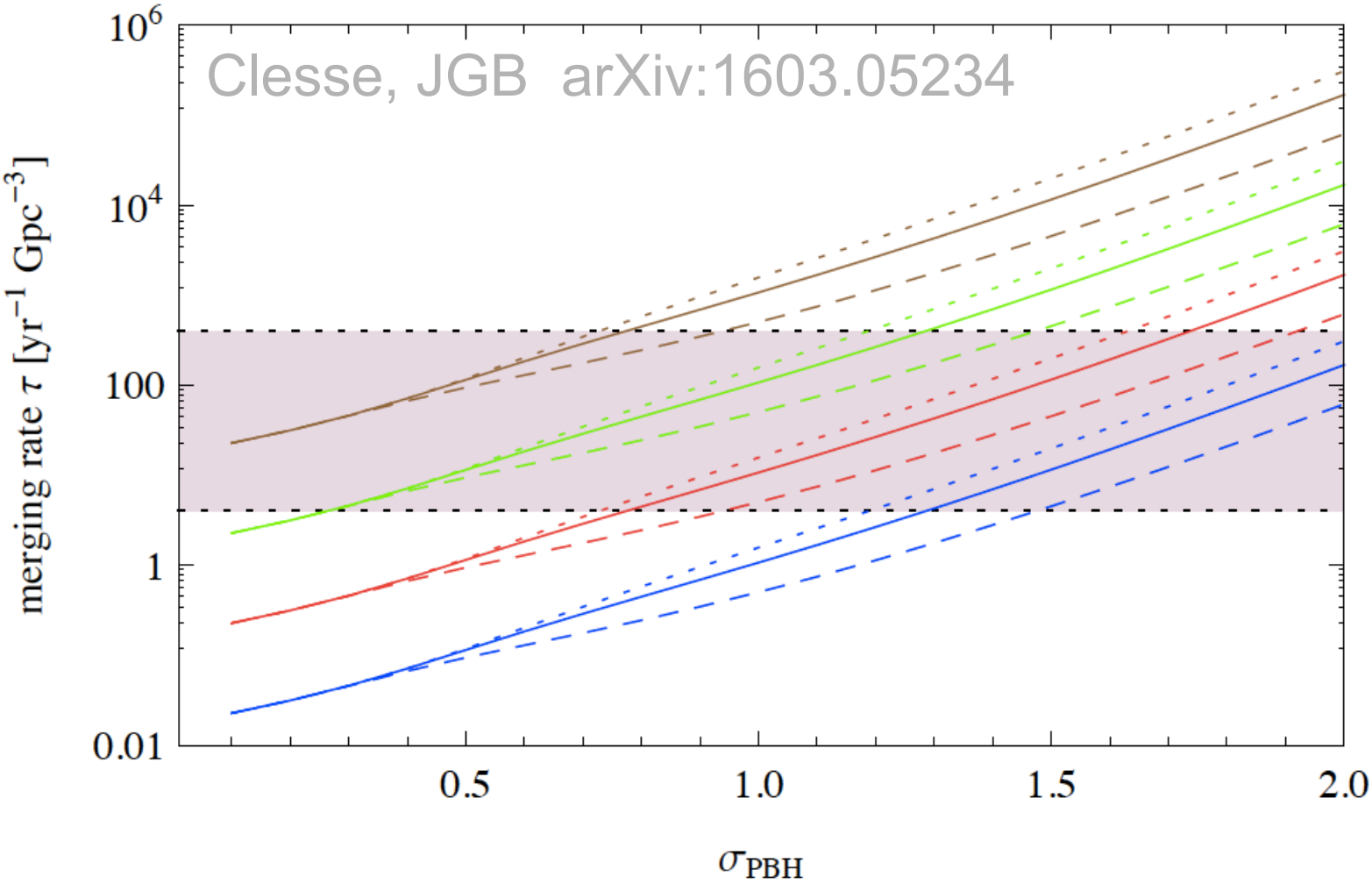

FIG. 2. Merging rate as a function of the width $\sigma_{\rm PBH}$ of the PBH density spectrum, for different values of the central mass of the distribution $\mu_{\rm PBH} = 10/30/60 M_\odot$ (respectively dotted, solid and dashed lines), and of the enhancement factor $E_{\rm factor} = 10^7/10^8/10^9/10^{10}$ (respectively blue, red, green and brown lines). The colored band corresponds to the bounds inferred by aLIGO.

Grav. Waves detections @ eLISA

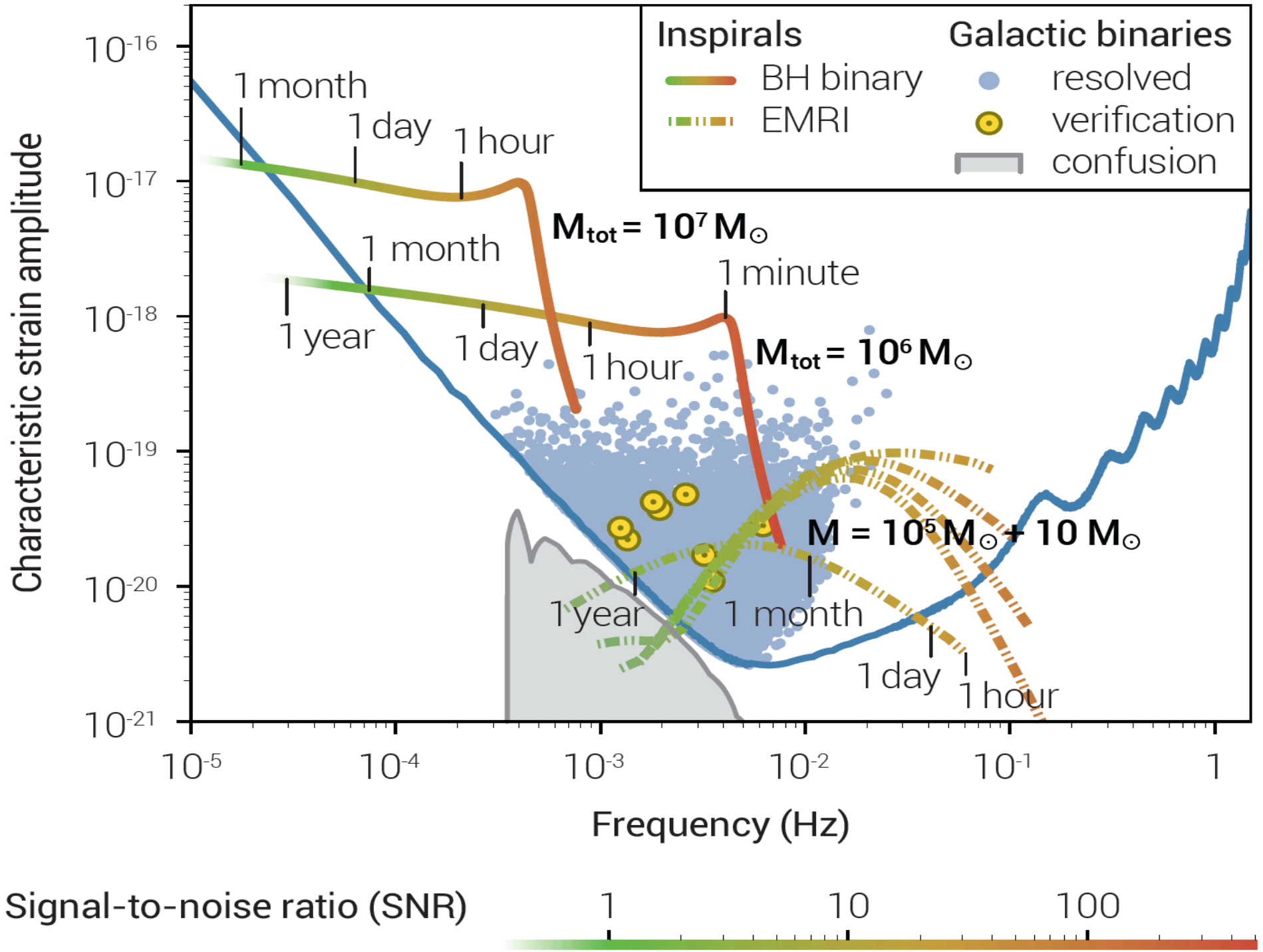
Inspirals
BH binary
EMRI
Galactic binaries
resolved
verification
confusion
Characteristic strain amplitude
Frequency (Hz)
10^{-16}
10^{-17}
10^{-18}
10^{-19}
10^{-20}
10^{-21}
10^{-5}
10^{-4}
10^{-3}
10^{-2}
10^{-1}
1
1 month
1 day
1 hour
$M_{tot} = 10^7 M_\odot$
1 month
1 minute
1 year
1 day
1 hour
$M_{tot} = 10^6 M_\odot$
$M = 10^5 M_\odot + 10 M_\odot$
1 year
1 month
1 day
1 hour
Signal-to-noise ratio (SNR)
1
10
100

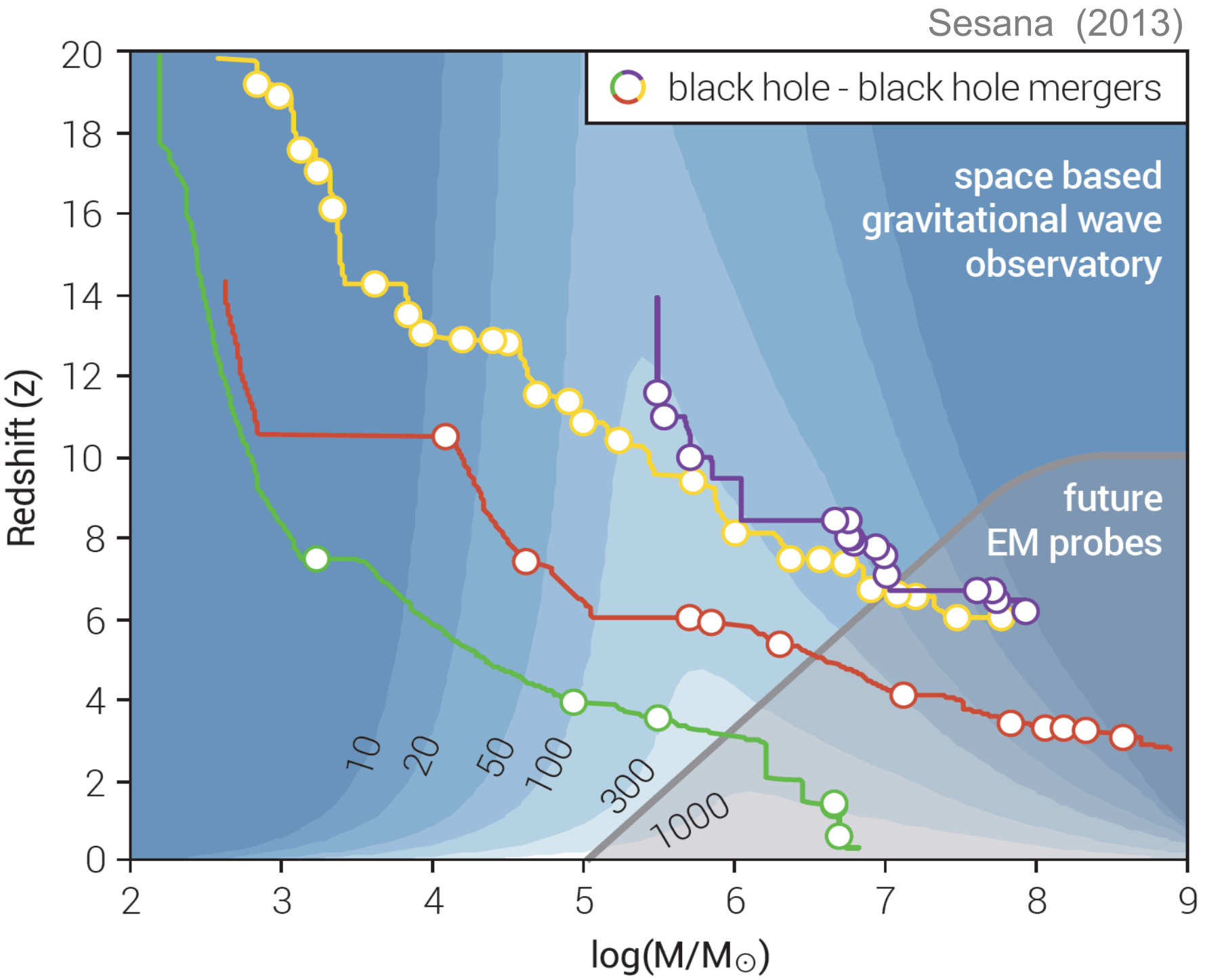
Sesana (2013)
black hole - black hole mergers
space based
gravitational wave
observatory
future
EM probes
10
20
50
100
300
1000
Redshift (z)
log(M/M⊙)
0
2
4
6
8
10
12
14
16
18
20
2
3
4
5
6
7
8
9

Stochastic Background Grav. Waves

Stochastic Background from MPBH

aLIGO arXiv:1602.03847

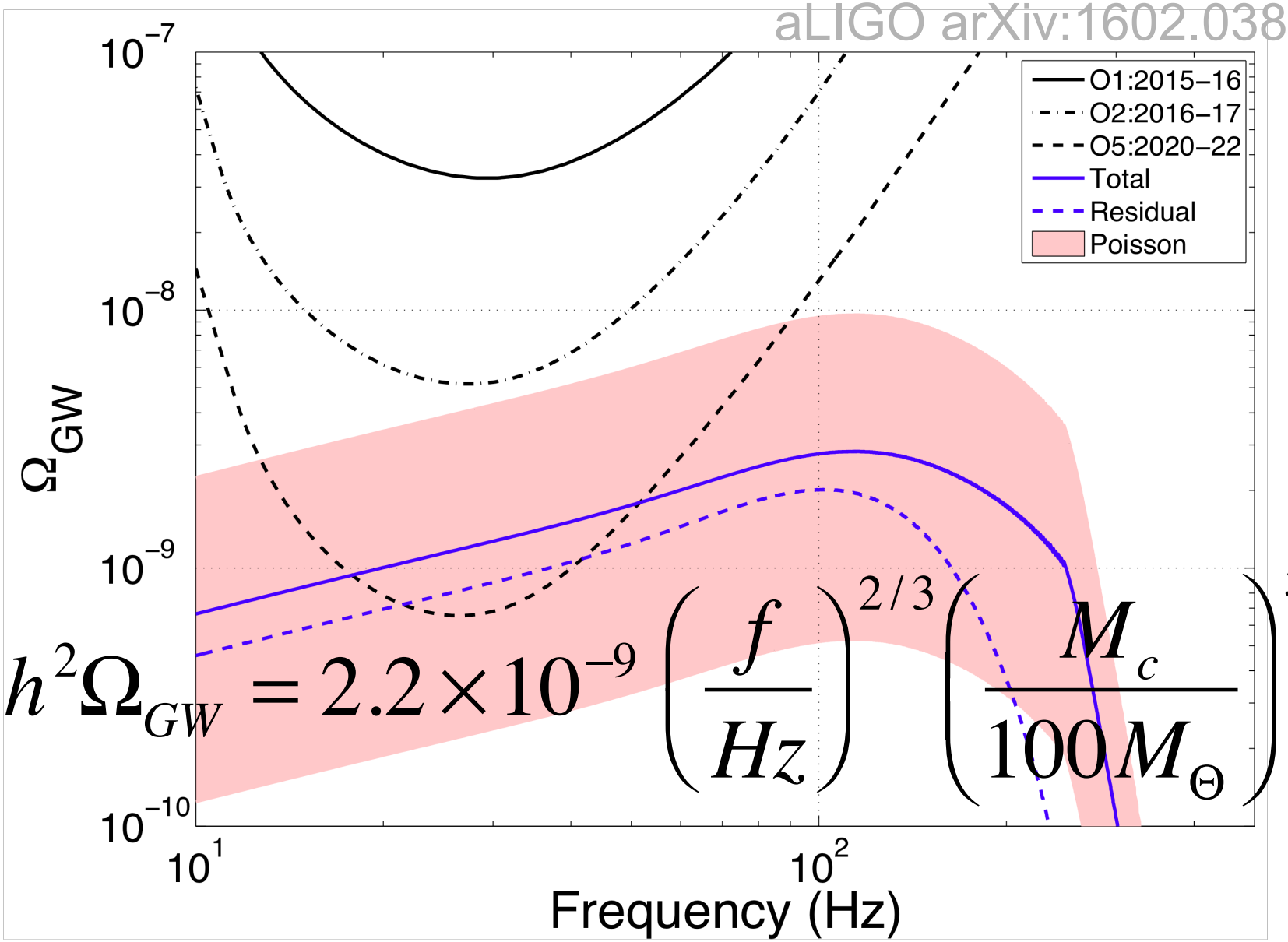

The Gravitational Wave Spectrum

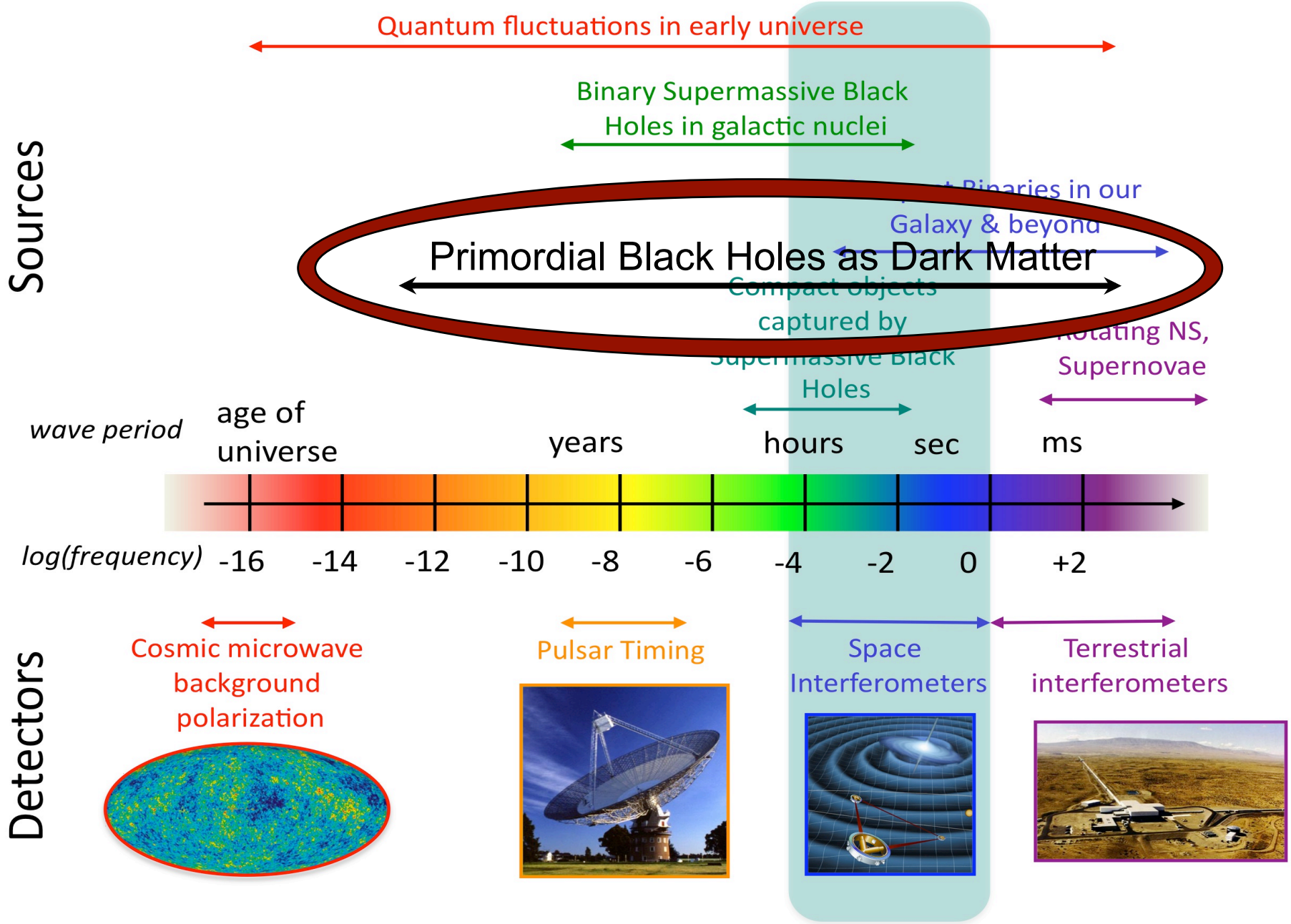

Sensitivity of future GW antenas

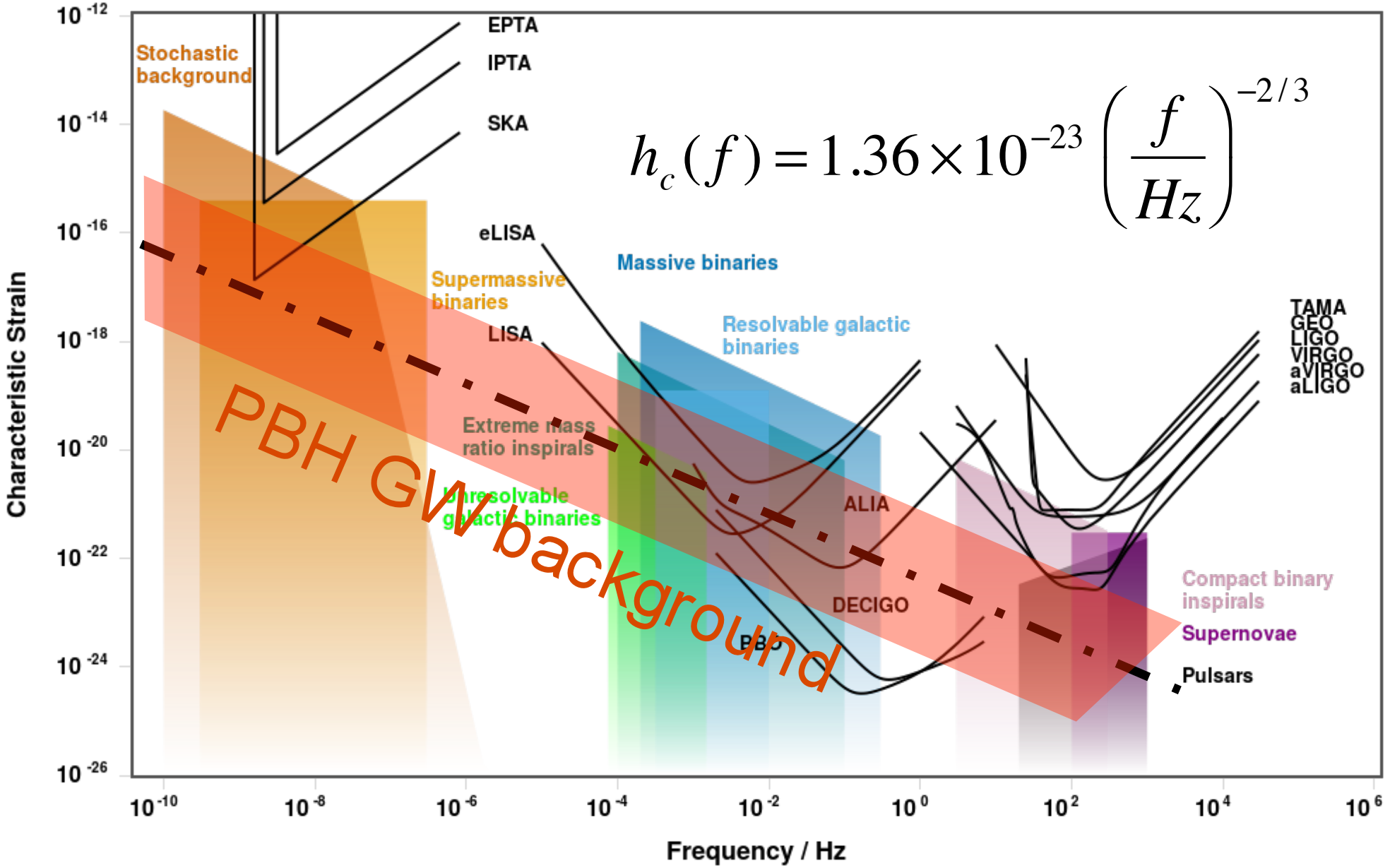

Discussion

Signatures of MPBH as DM

- Seeds of galaxies at high-z
- Reionization starts early (Kashlinsky)
- Larger galaxies form earlier than ΛCDM
- Massive BH at centers QSO @ z>6
- Growth of structure on small scales
- Ultra Luminous X-ray Transients
- MPBH in Andromeda (Chandra)
- GW from inspiraling BH (LIGO)
- Substructure and too-big-to-fail probl.
- Total integrated mass = Ω_M

Future tests

- GAIA positions and velocities of stars
- CMB distortions with CORE+
- GW from PBH mergers with LIGO
- Growth of structure on small scales
- Reionization history with SKA
- Direct detection from astrophysics (GAIA, X-rays and gamma-rays)
- SN or GRB femtolensing on MPBH
- Microlensing (long duration events)
- Stochastic Grav. Wave Background

Conclusions

- Massive Primordial Black Holes are the perfect candidates for CDM, in excellent agreement with CMB and LSS observations.
- MPBH could also resolve some of the most acute problems of ΛCDM paradigm, like early structure formation and substructure problems.
- MPBH open a new window into the Early Universe.
- There are many ways to test this idea in the near future from CMB, LSS, X-rays and GW.
- LISA could detect the stochastic background from MPBH merging since recombination.